



UNIVERSITÀ
DEGLI STUDI
DI PADOVA

Sede Amministrativa: Università degli Studi di Padova

Dipartimento di Medicina Molecolare - DMM

DOTTORATO DI RICERCA IN BIOMEDICINA
Curriculum in Medicina Rigenerativa
CICLO XXIX

**EXPERIMENTAL AND CLINICAL AIRWAY RESTORATION BY MESENCHYMAL STROMAL CELLS
AUTOLOGOUS ENDOSCOPIC TRANSPLANTATION**

Coordinatore : Ch.mo Prof. Stefano Piccolo

Supervisore :Ch.ma Prof.ssa Maria Teresa Conconi

(**firma** del Coordinatore e/o del Supervisore)

Dottorando : Francesco Petrella

(**firma** del dottorando)

CONTENTS

1. BRONCHO-PLEURAL FISTULA AND MESENCHYMAL STROMAL CELLS: CLINICAL BACKGROUND AND CURRENT PERSPECTIVES	8
1.1 Abbreviation list.....	8
1.2 Broncho-pleural fistula.....	8
1.3 Mesenchymal stromal cells	10
1.4 References	15
1.5 Figure Legend.....	19
2. EXPERIMENTAL AIRWAY RESTORATION: THE ANIMAL MODEL	22
2.1 Abbreviation list.....	22
2.2 Technology.....	22
2.3 Technique	23
2.4 “In vivo” experience	24
2.5 Comment	25
2.6 References	26
2.7 Figure Legend.....	27
3. CLINICAL AIRWAY RESTORATION: THE “FIRST-IN-HUMAN” EXPERIENCE	30
3.1 Abbreviation list.....	30
3.2 The recipient.....	30
3.3 Bone marrow aspiration.....	31
3.4 Stromal cell isolation, expansion and culture.....	32
3.5 MSC quality controls	33
3.6 Bronchoscopic implantation	34
3.7 Postoperative care and monitoring	35
3.8 Clinical and bronchoscopic findings	35
3.9 Cytohistopathology	36
3.10 Imaging	36
3.11 Comment	37
3.12 References	40
3.13 Figure Legend.....	41
4. “IN-VITRO” MSC TRACKING BY MAGNETIC RESONANCE IMAGING	46
4.1 Abbreviation list.....	46
4.2 Introduction	46

4.3 Materials and Methods	47
4.4 Results	50
4.5 Discussion	50
4.6 Acknowledgements.....	52
4.7 References	52
4.8 Tables and Figures Legends	54
5. FUTURE PERSPECTIVES: ADIPOSE DERIVED MESENCHYMAL STROMAL CELLS AND GRANULOCYTE-COLONY STIMULATING FACTOR FOR AIRWAY TISSUE DEFECTS	58
5.1 Abbreviation List	58
5.2 Clinical background	58
5.3 Preliminary data.....	59
5.4 Experimental design aim 1	61
5.5 Experimental design aim 2	61
5.6 Experimental design aim 3	59
5.7 Methodologies and statistical analyses.....	62
5.8 Expected outcomes.....	63
5.9 Risk analysis, possible problems and solutions.....	63
5.10 Significance and innovation	64
5.11 References	65
5.12 Figure Legend.....	67

“The prime goal is to alleviate suffering, and not to prolong life. If your treatment does not alleviate suffering, but only prolongs life, that treatment should be stopped.”

Christiaan Neethling Barnard

Pioneer cardiac surgeon

“There is no finish line in the work of science. The race is always with us – the urgent work of giving substance to hope and answering those many bedside prayers, of seeking a day when words like "terminal" and "incurable" are finally retired from our vocabulary.”

Barack Hussein Obama II

President of the United States of America

SUMMARY

Post resectional broncho-pleural fistula is a pathological connection between the airways and the pleural space that may develop after lung resection. It may be caused by incomplete bronchial closure, impediment of bronchial stump wound healing, or stump destruction by residual neoplastic tissue; its mortality ranges from 12.5 to 71.2%, therefore it is still the most feared complication after curative lung resection; for this reason the healing effects promoted by stem cells – by transformation into mature cells with a specialized function or by enhancing intrinsic repair mechanisms –may represent an effective and only partially explored therapeutic option . Mesenchymal stromal cells have the ability to migrate and engraft at sites of inflammation and injury in response to cytokines, chemokines, and growth factors at a wound site and they can exert local reparative effects through transdifferentiation into tissue-specific cell types or via the paracrine secretion of soluble factors with anti-inflammatory and wound-healing activities.

We proposed, on an animal model, an autologous bone marrow derived mesenchymal stromal cells transplantation: it allowed bronchial stump healing by extraluminal fibroblast proliferation and collagenous matrix development. Encouraged by experimental bronchial wall restoration in large animals and by functional human organ replacement elsewhere, we undertook autologous bone marrow derived mesenchymal stromal cells bronchoscopic transplantation to treat a patient who developed broncho-pleural fistula. The bronchoscopic transplantation of bone marrow-derived mesenchymal stromal cells in our patient appeared to help close this small-caliber post resectional broncho-pleural fistula, further boosting regenerative medicine approach for airway diseases.

Considering the need to specifically track mesenchymal stromal cells following transplantation in order to evaluate different method of implantation, to follow their migration within the body and to quantify their accumulation at the target, we proposed magnetic resonance imaging tracking both by superparamagnetic

iron oxide particles and perfluorocarbon nanoemulsion formulations , demonstrating that were both effective, without altering cell viability or differentiation.

Finally we proposed adipose derived mesenchymal stromal cells bronchoscopic transplantation and intra venous injection of Granulocyte Colony Stimulating Factors as a faster method and a new frontier in airway restoration.

RIASSUNTO

La fistola bronco pleurica post chirurgica è una comunicazione patologica fra le vie aeree e lo spazio pleurico che puo' verificarsi dopo resezione polmonare. Essa puo' essere causata da chiusura bronchiale incompleta, da alterazioni della cicatrizzazione del moncone bronchiale o dalla distruzione del moncone da parte di tessuto neoplastico residuo.

La sua mortalità varia dal 12.5 al 71.2%, rendendola ancora oggi la piu' temuta complicanza dopo resezione polmonare; per tale ragione, l'effetto cicatriziale promosso dalle cellule staminali – tramite la trasformazione in cellule mature con una specifica funzione o tramite l'implementazione di meccanismi intrinseci di riparazione – potrebbe rappresentare una opzione terapeutica efficace e, ad oggi , solo parzialmente esplorata. Le cellule mesenchimali stromali hanno la capacità di migrare ed attecchire a siti di infiammazione e danno tissutale, in risposta a citochine, chemochine e fattori di crescita e possono esercitare un'azione riparativa locale attraverso un'azione di transdifferenziazione o attraverso un'azione di secrezione paracrina di fattori solubili con proprietà antiinfiammatori e procicatriziali.

Noi abbiamo proposto, su di un modello animale , un trapianto autologo di cellule stromali mesenchimali di derivazione midollare: questo ha permesso una cicatrizzazione del moncone bronchiale grazie alla proliferazione di fibroblasti ed all'apposizione di matrice collagene. Incoraggiati dalla riparazione delle vie aeree sul modello di grande animale abbiamo utilizzato tale metodica per trattare un paziente che aveva sviluppato una fistola bronco pleurica. Il trapianto broncoscopico di cellule stromali mesenchimali midollari

si è rivelato efficace – nel nostro caso clinico – nella chiusura di una piccola fistola post chirurgica, stimolando ulteriormente l'approccio di medicina rigenerativa anche per problemi di vie aeree.

Considerando la necessità di marcare le cellule stromali mesenchimali dopo un trapianto cellulare, al fine di valutare differenti metodi di impianto, di seguire la loro migrazione nel corpo e di quantificare il loro accumulo al sito bersaglio, abbiamo proposto la risonanza magnetica nucleare come metodo per la marcatura cellulare, sia con mezzi di contrasto superparamagnetici che con formulazioni di nanoemulsioni con fluoro, osservando come entrambe si siano dimostrate efficaci, senza tuttavia alterare la biodisponibilità cellulare o la loro differenziazione.

Infine, abbiamo proposto l'impiego di cellule stromali mesenchimali insieme alla somministrazione di G-CSF come metodo piu' rapido e nuova frontiera nella riparazione delle vie aeree.

1. BRONCHO-PLEURAL FISTULA AND MESENCHYMAL STROMAL CELLS: CLINICAL BACKGROUND AND CURRENT PERSPECTIVES

1.1 Abbreviation list

BPF: broncho-pleural fistula

MSC: mesenchymal stromal cell

BM-MSC: bone marrow-MSC

AT-MSC: adipose tissue-MSC

MHC: Major Histocompatibility Complex

IL-10: Interleukin-10

IL-6: Interleukin-6

TGFB: Transforming Growth Factor Beta,

VEGF: Vascular Endothelial Growth Factor

ICAMs: Intercellular Adhesion Molecules

PG E2: Prostaglandin E2

EGFR: epidermal growth factor receptor

BASC: bronchoalveolar stem cells

1.2 Broncho-pleural fistula

Post resectional broncho-pleural fistula (BPF) is a pathological connection between the airways and the pleural space that may develop after lung resection **[Figure 1] [1]**. It may be caused by incomplete bronchial closure, impediment of bronchial stump wound healing, or stump destruction by residual neoplastic tissue. The incidence of BPF after thoracic surgery for lung cancer ranges from 1 to 4%, whilst its mortality ranges from 12.5 to 71.2% **[2]**.

BPF is still the most feared complication after curative lung resection [3]; for this reason the healing effects promoted by stem cells – by transformation into mature cells with a specialized function or by enhancing intrinsic repair mechanisms – may represent an effective and only partially explored therapeutic option [4, 5]. There is still a lack of consensus about the optimal management of the BPF, but individualized approach is usually recommended [6].

Several strategies have been employed to manage the problem with variable success: surgery, direct closure with re-enforcement of pleural, pericardial, intercostal or omental flaps may be necessary; as a less invasive option, fibrin glue has been used by several investigators [7]. A post-surgical broncho-pleural fistula is more common in patients with inflammatory broncho-pulmonary diseases, particularly active tuberculosis. Preoperative risk factors for the development of BPF are: fever, steroid use, elevated erythrocyte sedimentation rate and anemia; postoperative risk factors are: fever, steroid use, leukocytosis, tracheostomy and prolonged mechanical ventilation, repeated bronchoscopy for sputum suction and mucus plugging [8]. Further risk factors meriting to be mentioned are an extensive mediastinal lymphadenectomy, ageing, and preoperative chemotherapy and radiotherapy.

BPF is more common after pneumonectomy than following lesser resection and it is more common after right-sided operation than left pneumonectomy; moreover, BPF occurring after pneumonectomy is clinically more devastating than after lobectomy or segmentectomy [9]. BPF is more common after resections for inflammatory disease of the lung, especially in patients with active tuberculosis and positive sputum. A BPF can occur at any time during the postoperative period but more frequently occurs within 8 to 12 days after surgery; if seen within the first week after surgery, BPF may be due to a mechanical failure of closure of the stump and requires surgical exploration and an attempt of reclosure.

The clinical presentation of post-surgical broncho-pulmonary fistula may be acute, subacute or chronic. The clinical presentation of a BPF may be acute, subacute, or chronic. The acute BPF is a life-threatening condition due to tension pneumothorax or asphyxiation from pulmonary flooding. The patient has dyspnea, subcutaneous emphysema, cough with expectoration of fluid or purulent material. There is mediastinal

shifting on radiological images [6]. The subacute form is characterized by wasting, malaise, fever and minimally productive cough; the presence of fibrosis in the pleural space is usually associated with this form preventing the mediastinal shift [6]. Chronic BPF presents with fever, productive cough and new or increasing air fluid levels on the chest X-ray; in case of chronic tracheo-esophageal fistula, coughing and dyspnea are preferably observed during drinking and eating [6].

From the beginning of modern thoracic surgery, many complex procedures have been advocated as salvage therapy for broncho-pleural fistula: muscle flap closure, completion lobectomy or pneumonectomy, and thoracoplasty are only some examples of the surgical options; open window thoracostomy – consisting of rib resection and daily medications by gauzes – is one of the most effective rescue treatments, but on the other hand, it is one of the most aggressive and psychologically disabling operations a patient can undergo [Figure 2].

With the advent of flexible bronchoscopy, a plethora of endoscopic treatments have been proposed for broncho-pleural fistula closure, fibrin glue local injection and stenting being the most reported in the literature. Recently, mesenchymal stromal cell endoscopic transplantation is one of the most promising treatment of BPF [10]. Nevertheless, only small caliber fistula can be managed by a pure bronchoscopic approach, given that the failure rate may be not negligible and so - although cellular therapies may represent a new interesting therapeutic option for airway fistula closure - before they can be routinely used as a treatment, more basic research and clinical experiences needed.

1.3 Mesenchymal stromal cells

Mesenchymal stromal cells (MSCs) [Figure 3] are a population of undifferentiated multipotent adult cells that naturally reside within the human body and are generally defined as plastic-adherent, fibroblast-like cells possessing extensive self-renewal properties and potential to differentiate *in vivo* and *in vitro* into a variety of mesenchymal lineage cells [11]; they can differentiate into osteogenic, chondrogenic, and

adipogenic lineages when cultured in specific inducing media [12]. MSCs are described as Major Histocompatibility Complex II (MHC II) negative cells, lacking costimulatory molecules such as CD40, CD80, and CD86, thus having an immune phenotype (MHC II⁻, CD40⁻, and CD86⁻) allowing evading the host immune system, thus permitting allogenic transplantation without immunosuppression [13].

The immunomodulatory and anti-inflammatory effect of MSCs have been extensively studied and used in the gastrointestinal tract, like in inflammatory bowel disease and graft versus- host disease [14,15]; it has been recently demonstrate that MSCs derived from Crohn's patients deploy indoleamine 2,3-dioxygenase-mediated immune suppression [16]. Once implanted, MSCs are able to interact with the surrounding microenvironment, promoting tissue healing and regeneration, renewing biologic function by supportive and trophic functions based on cross talk with other cells present within diseased tissues [17].

MSCs have been shown to exert profound anti-inflammatory and immunomodulatory effects on almost all the cells of the innate and adaptative immune system by a variety of mechanisms, notably cytokine and chemokine secretion, like Interleukin-10 (IL-10), Interleukin 6 (IL-6), Transforming Growth Factor Beta (TGFB), Vascular Endothelial Growth Factor (VEGF), Intercellular Adhesion Molecules (ICAMs), and Prostaglandin E2 (PG E2) [18].

After their initial discovery in bone marrow, MSCs were isolated and characterized from a wide variety of other adult and fetal tissue, including adipose tissue [19], umbilical cord [20], dental pulp [21], tendon [22], thymus, spleen [23], cornea [24], liver [25], brain [26], periosteum [27], placenta [28], and synovial and amniotic fluids [29]. MSCs isolated from these different tissues are different, although no significant difference in the profiles of secreted cytokines by different type of MSCs has been described; some quantitative differences in the cytokine secretions by adipose tissue-derived MSCs (AT-MSCs) and bone marrow-derived MSC (BM-MSC) have been reported [30].

Besides the trilineage differentiation potential into osteoblasts, adipocytes, and chondroblasts in in vitro culture with specific stimuli, experimental data have demonstrated that MSCs can also differentiate into other mesodermal lineages, such as skeletal myocytes, cardiomyocytes, tenocytes, and endothelial cells;

moreover MSCs have the capacity to differentiate into types of cells of endodermal and ectodermal lineages, including hepatocytes, neuronal cells with neuron-like functions, insulin-producing cells, photoreceptor cells, renal tubular epithelial cells, and epidermal and sebaceous duct cells [18].

MSCs have the ability to migrate and engraft at sites of inflammation and injury in response to cytokines, chemokines, and growth factors [31] at a wound site and they can exert local reparative effects through transdifferentiation into tissue-specific cell types or via the paracrine secretion of soluble factors with anti-inflammatory and wound-healing activities [32].

The lung is a highly quiescent tissue, previously thought to have limited reparative capacity and a susceptibility to scarring [33]; we now know that the lung has a remarkable reparative capacity, when needed, in response to specific stimuli and injuries [34].

The tissues of the lung may be categorized as having facultative progenitor cell populations that can be induced to proliferate in response to injury as well as differentiate into one or more cell types; given the complexity of the respiratory system, a single lung stem cell generating all of the various lineages within the lung is difficult to conceive: the two most likely hypotheses are that the lung could respond to injury and stress (a) by activating stem cell populations or (b) by reentering the cell cycle to repopulate lost cells [34].

During lung embryonic development, rapid proliferation and differentiation are the rule rather than the exception; on the contrary, in the adult lung during postnatal life, it is not clear whether any lung cells of comparably expansive proliferative potential or differentiation repertoire still remain active, and so we refer to these developing cells as progenitors rather than stem cells, as their self-renewal capacity may be transient [34]. We can identify, within the respiratory system, at least four different districts in which different stem cell candidates may be considered: (1) trachea and proximal bronchi, (2) distal airway system, (3) alveolar compartment, and (4) bronchoalveolar duct junction. The trachea and main stem bronchi are lined with pseudostratified epithelium composed of basal and luminal cells; subsets of basal cells, both in mice and in humans, have extensive proliferative potential, self-renewal capacity, and the ability to differentiate into basal, secretory, and ciliated lung epithelial cells in vivo [35]; considering that

basal cells have no other known function in the lung, this supports the concept that basal cells can function as tissue-specific stem cells of the airway epithelium, although little is known about basal cell self-renewal and differentiation and whether it involves asymmetric cell division as do other stem cells [34]. In the distal airway the bronchiolar epithelium is quiescent until injured; a subset of secretory cells, named variant club cells, show proliferation potential in response to injury but it is still unclear if they go through a process of dedifferentiation to reenter the cell cycle and then differentiate again after expansion [36]; these cells can be found adjacent to the neuroendocrine bodies or at the bronchoalveolar duct junction, confirming the hypothesis of the existence of microenvironmental progenitor cell niches in the airways [10].

The type II alveolar epithelial cells are considered the best candidate for progenitor cells of the adult lung alveolus [37] during the late development, in fact, or after various postnatal alveolar injuries; some type II alveolar epithelial cells can proliferate, self-renew, and form alveolar epithelial cells type I presenting self-renewal signals like epidermal growth factor receptor (EGFR) [38].

At the transition from the bronchiolar region to the alveolar region of the lung there is the bronchoalveolar duct junction, where some variant club cells possess airway epithelial regenerative potential after induced lung injury [34], defined as bronchoalveolar stem cells (BASC); however the existence of BASC *in vivo* has been contested [39] so further studies are required to consider BASC as true stem cell lineage existing in a unique niche between the airways and alveoli [34].

The main function of stem/progenitor cells for the airway epithelium is epithelial homeostasis and the repair of defects in the airway wall [40]. Stem/progenitor cells can be used to repair defects in the airway wall, resulting from tumors, trauma, tissue reactions following long-time intubations, or diseases that are associated with epithelial damage [41]. In many airways diseases such as asthma, chronic obstructive pulmonary diseases, obliterative bronchiolitis, and cystic fibrosis, the airway epithelium is damaged and subsequently repaired and remodeled [42]. Reconstruction of tracheobronchial defects requires in the first place the availability of airway epithelial cells and the presence of fibroblasts or fibroblast-derived substances.

The fact that fibroblasts have positive effects on airway epithelial cell growth emphasizes the fact that the airway is not a simple structure and that epithelial-mesenchymal interactions are important. Considering the catastrophic consequences that airway tissue defects may have after lung resection, culminating in a pathological communication between the airways and the pleural space called “broncho-pleural fistula” (BPF), we proposed, on an animal model, an autologous bone marrow derived mesenchymal stromal cells (BMMSC) transplantation: it allowed bronchial stump healing by extraluminal fibroblast proliferation and collagenous matrix development [1]. Encouraged by experimental bronchial wall restoration in large animals and by functional human organ replacement elsewhere [43], we undertook autologous BMMSC bronchoscopic transplantation to treat a patient who developed BPF after right extrapleural pneumonectomy for malignant mesothelioma [10]. The bronchoscopic transplantation of bone marrow-derived mesenchymal stromal cells in our patient appeared to help close this small-caliber post resectional broncho-pleural fistula, further boosting regenerative medicine approach for airway diseases. There are a number of ongoing clinical trials addressing the feasibility and safety of MSCs treatment for airway diseases, focusing on the role of human MSCs for the treatment of subjects with moderate to severe chronic obstructive pulmonary disease [44,45].

1.4 References

1. Petrella F, Toffalorio F, Brizzola S, De Pas TM, Rizzo S, Barberis M, Pelicci P, Spaggiari L, Acocella F. Stem cell transplantation effectively occludes broncho-pleural fistula in an animal model. *Ann Thorac Surg*. 2014 Feb;97(2):480–3.
2. Sonobe M, Nakagawa M, Ichinose M, Ikegami N, Nagasawa M, Shindo T. Analysis of risk factors in broncho-pleural fistula after pulmonary resection for primary lung cancer. *Eur J Cardiothorac Surg*. 2000;18:519–23.
3. Gomez-de-Antonio D, Zurita M, Santos M, Salas I, Vaquero J, Varela A. Stem cells and bronchial stump healing. *J Thorac Cardiovasc Surg*. 2010;140:1397–401.
4. Wu Y, Chen L, Scott PG, Tredget EE. Mesenchymal stem cells enhance wound healing through differentiation and angiogenesis. *Stem Cells*. 2007;25:2648–59.
5. Mellough CB, Sernagor E, Moreno-Gimeno I, Steel DH, Lako M. Efficient stage-specific differentiation of human pluripotent stem cells toward retinal photoreceptor cells. *Stem Cells*. 2012;30:673–86.
6. Lois M, Noppen M. Broncho-pleural fistulas: An overview of the problem with special focus on endoscopic management. *Chest*. 2005;128:3955–65.
7. Shrestha P, Safdar SA, Jawad SA, Shaaban H, Dieguez J, Elberaqqdar E, Rai S, Adelman M. Successful closure of a broncho-pleural fistula by intrapleural administration of fibrin sealant: a case report with review of literature. *N Am J Med Sci*. 2014 Sep;6(9):487–90.
8. Sato M, Saito Y, Fujimura S, Usuda K, Takahashi S, Kanma K, Imai S, Suda H, Nakada T, Hashimoto K. Study of postoperative broncho-pleural fistulas: analysis of factors related to broncho-pleural fistulas. *Nippon kyobu Geka Gekai Zasshi*. 1989;37:498–503.
9. Ponn, RB. *General Thoracic Surgery*. Sixth Edition. Vol. 1. Lippincott Williams & Wilkins; Complications of pulmonary resection; pp. 554–586. Chapter 37.

10. Petrella F, Spaggiari L, Acocella F, Barberis M, Bellomi M, Brizzola S, Donghi S, Giardina G, Giordano R, Guarize J, Lazzari L, Montemurro T, Pastano R, Rizzo S, Toffalorio F, Tosoni A, Zanotti M. Airway fistula closure after stem-cell infusion. *N Engl J Med*. 2015 Jan 1;372(1):96–7.
11. M. F. Pittenger, A. M. Mackay, S. C. Beck et al., “Multilineage potential of adult human mesenchymal stem cells,” *Science*, vol. 284, no. 5411, pp. 143–147, 1999.
12. G. Siegel, R. Schöfer, and F. Dazzi, “The immunosuppressive properties of mesenchymal stem cells,” *Transplantation*, vol. 87, pp. S45–S49, 2009.
13. K. Igura, X. Zhang, K. Takahashi, A. Mitsuru, S. Yamaguchi, and T. A. Takahashi, “Isolation and characterization of mesenchymal progenitor cells from chorionic villi of human placenta,” *Cytotherapy*, vol. 6, no. 6, pp. 543–553, 2004.
14. M. J. Hoogduijn, “Are mesenchymal stromal cells immune cells?” *Arthritis Research & Therapy*, vol. 17, no. 1, article 88, 2015.
15. K. Nagaishi, Y. Arimura, and M. Fujimiya, “Stem cell therapy for inflammatory bowel disease,” *Journal of Gastroenterology*, vol. 50, no. 3, pp. 280–286, 2015.
16. R. Chinnadurai, I. B. Copland, S. Ng et al., “Mesenchymal stromal cells derived from Crohn’s patients deploy indoleamine 2,3-dioxygenase mediated immune suppression, independent of autophagy,” *Molecular Therapy*, 2015.
17. S. Baiguera, P. Jungebluth, B. Mazzanti, and P. Macchiarini, “Mesenchymal stromal cells for tissue-engineered tissue and organ replacements,” *Transplant International*, vol. 25, no. 4, pp. 369–382, 2012.
18. D. Kyurkchiev, I. Bochev, E. Ivanova-Todorova et al., “Secretion of immunoregulatory cytokines by mesenchymal stem cells,” *World Journal of Stem Cells*, vol. 6, no. 5, pp. 552–570, 2014.
19. S. Kern, H. Eichler, J. Stoeve, H. Klüter, and K. Bieback, “Comparative analysis of mesenchymal stem cells from bone marrow, umbilical cord blood, or adipose tissue,” *Stem Cells*, vol. 24, no. 5, pp. 1294–1301, 2006.

20. C. Capelli, E. Gotti, M. Morigi et al., "Minimally manipulated whole human umbilical cord is a rich source of clinical-grade human mesenchymal stromal cells expanded in human platelet lysate," *Cytotherapy*, vol. 13, no. 7, pp. 786–801, 2011.
21. S. Gronthos, "The therapeutic potential of dental pulp cells: more than pulp fiction?" *Cytotherapy*, vol. 13, no. 10, pp. 1162–1163, 2011.
22. Y. Bi, D. Ehrchiou, T. M. Kilts et al., "Identification of tendon stem/progenitor cells and the role of the extracellular matrix in their niche," *Nature Medicine*, vol. 13, no. 10, pp. 1219–1227, 2007.
23. M. Krampera, S. Sartoris, F. Liotta et al., "Immune regulation by mesenchymal stem cells derived from adult spleen and thymus," *Stem Cells and Development*, vol. 16, no. 5, pp. 797–810, 2007.
24. P.-F. Choong, P.-L. Mok, S.-K. Cheong, and K.-Y. Then, "Mesenchymal stromal cell-like characteristics of corneal keratocytes," *Cytotherapy*, vol. 9, no. 3, pp. 252–258, 2007.
25. M. Najimi, D. N. Khuu, P. A. Lysy et al., "Adult-derived human liver mesenchymal-like cells as a potential progenitor reservoir of hepatocytes?" *Cell Transplantation*, vol. 16, no. 7, pp. 717–728, 2007.
26. S.-G. Kang, N. Shinojima, A. Hossain et al., "Isolation and perivascular localization of mesenchymal stem cells from mouse brain," *Neurosurgery*, vol. 67, no. 3, pp. 711–720, 2010.
27. H. Nakahara, S. P. Bruder, S. E. Haynesworth et al., "Bone and cartilage formation in diffusion chambers by subcultured cells derived from the periosteum," *Bone*, vol. 11, no. 3, pp. 181–188, 1990.
28. V. Sabapathy, S. Ravi, V. Srivastava, A. Srivastava, and S. Kumar, "Long-term cultured human term placenta-derived mesenchymal stem cells of maternal origin displays plasticity," *Stem Cells International*, vol. 2012, Article ID 174328, 11 pages, 2012.
29. P. Lotfinejad, K. Shamsasenjan, A. Movassaghpour, J. Majidi, and B. Baradaran, "Immunomodulatory nature and site specific affinity of mesenchymal stem cells: a hope in cell therapy," *Advanced Pharmaceutical Bulletin*, vol. 4, no. 1, pp. 5–13, 2014.

30. C. W. Park, K.-S. Kim, S. Bae et al., "Cytokine secretion profiling of human mesenchymal stem cells by antibody array," *International Journal of Stem Cells*, vol. 2, no. 1, pp. 59–68, 2009.
31. D.-C. Ding, W.-C. Shyu, and S.-Z. Lin, "Mesenchymal stem cells," *Cell Transplantation*, vol. 20, no. 1, pp. 5–14, 2011.
32. Y. Wu, L. Chen, P.G. F. Scott, and E. E. Tredget, "Mesenchymal stem cells enhance wound healing through differentiation and angiogenesis," *Stem Cells*, vol. 25, no. 10, pp. 2648–2659, 2007.
33. M. F. Beers and E. E. Morrisey, "The three R's of lung health and disease: repair, remodeling, and regeneration," *Journal of Clinical Investigation*, vol. 121, no. 6, pp. 2065–2073, 2011.
34. D. N. Kotton and E. E. Morrisey, "Lung regeneration: mechanisms, applications and emerging stemcell populations," *Nature Medicine*, vol. 20, no. 8, pp. 822–832, 2014.
35. J. R. Rock, M. W. Onaitis, E. L. Rawlins et al., "Basal cells as stem cells of the mouse trachea and human airway epithelium," *Proceedings of the National Academy of Sciences of the United States of America*, vol. 106, no. 31, pp. 12771–12775, 2009.
36. R. J. Mason and M. C. Williams, "Type II alveolar cell. Defender of the alveolus," *The American Review of Respiratory Disease*, vol. 115, no. 6, pp. 81–91, 1977.
37. A.-K. T. Perl, S. E. Wert, A. Nagy, C. G. Lobe, and J. A. Whitsett, "Early restriction of peripheral and proximal cell lineages during formation of the lung," *Proceedings of the National Academy of Sciences of the United States of America*, vol. 99, no. 16, pp. 10482–10487, 2002.
38. T. J. Desai, D. G. Brownfield, and M. A. Krasnow, "Alveolar progenitor and stem cells in lung development, renewal and cancer," *Nature*, vol. 507, no. 7491, pp. 190–194, 2014.
39. E. L. Rawlins, T. Okubo, Y. Xue et al., "The role of Scgb1a1+ Clara cells in the long-term maintenance and repair of lung airway, but not alveolar, epithelium," *Cell Stem Cell*, vol. 4, no. 6, pp. 525–534, 2009.

40. A. Giangreco, E. N. Arwert, I. R. Rosewell, J. Snyder, F. M. Watt, and B. R. Stripp, "Stem cells are dispensable for lung homeostasis but restore airways after injury," *Proceedings of the National Academy of Sciences of the United States of America*, vol. 106, no. 23, pp. 9286–9291, 2009.
41. G. M. Roomans, "Tissue engineering and the use of stem/progenitor cells for airway epithelium repair," *European Cells and Materials*, vol. 19, pp. 284–299, 2010.
42. C. Coraux, J. Roux, T. Jolly, and P. Birembaut, "Epithelial cell-extracellular matrix interactions and stem cells in airway epithelial regeneration," *Proceedings of the American Thoracic Society*, vol. 5, no. 6, pp. 689–694, 2008.
43. P. Diaz-Agero Alvarez, M. Garcia-Arranz, T. Georgiev-Hristov, and D. Garcia-Olmo, "A new bronchoscopic treatment of tracheomediastinal fistula using autologous adipose-derived stem cells," *Thorax*, vol. 63, no. 4, pp. 374–376, 2008.
44. <https://clinicaltrials.gov/ct2/show/NCT00683722>.
45. <https://clinicaltrials.gov/ct2/show/NCT02041000>.

1.5 Figure Legend

Figure 1: bronchoscopic view of post resectional broncho-pleural fistula

Figure 2: open window thoracostomy before (a) and after (b) filling in by gauzes

Figure 3: human mesenchymal stromal cells at passage 1

Figure 1: bronchoscopic view of post resectional broncho-pleural fistula

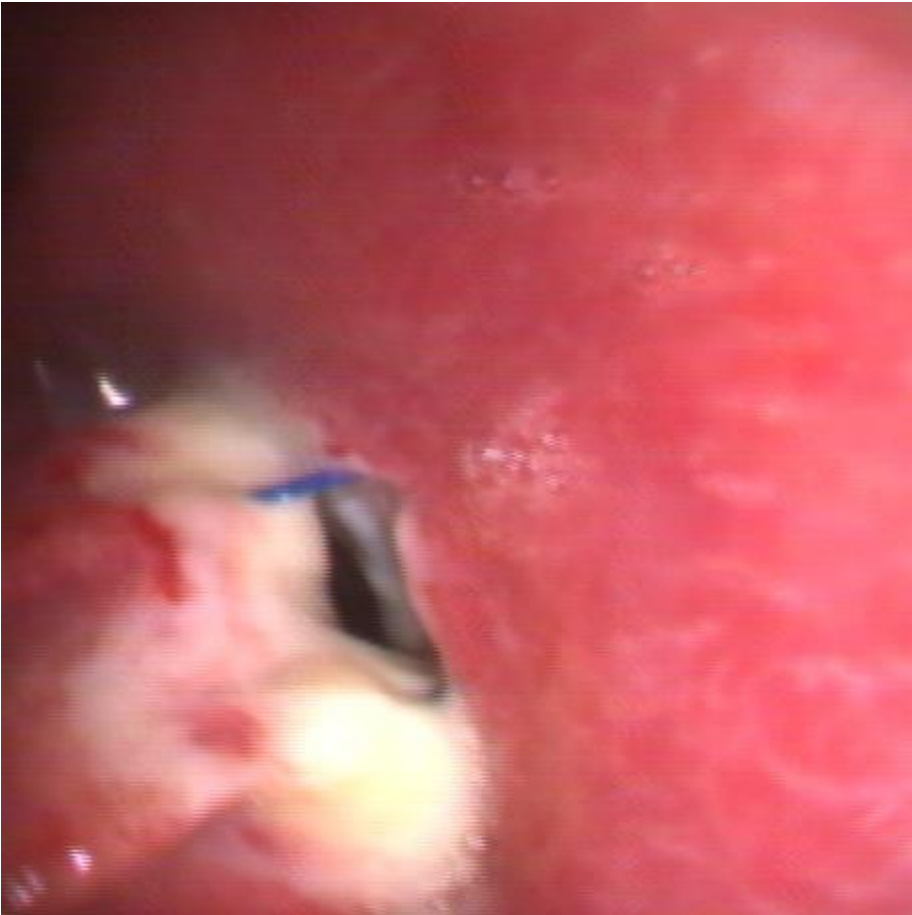
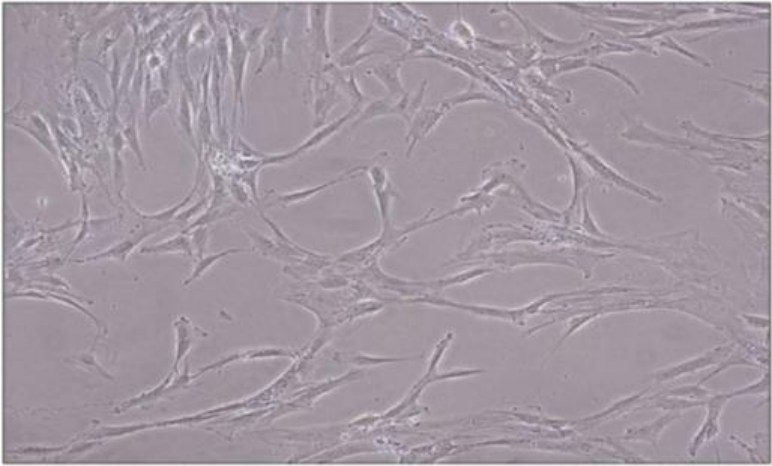


Figure 2: open window thoracostomy before (a) and after (b) filling in by gauzes



Figure 3: human mensenchymal stromal cells at passage 1



2. EXPERIMENTAL AIRWAY RESTORATION: THE ANIMAL MODEL

2.1 Abbreviation list

CT: computed tomography

MRI: magnetic resonance imaging

Our project investigates the hypothesis of experimental BPF closure by bronchoscopic injection of autologous bone marrow-derived mesenchymal stromal cells (MSC) into the cavity of the fistula, evaluating its feasibility and safety in a large animal model.

2.2 Technology

Animals were treated according the requirements of the European Union Directive 86/609 regarding the protection of animals used for experimental or other scientific purpose and the Council of Europe Convention for the protection of vertebrate animals used for experimental and other scientific purpose (ETS 123).

The present study was performed in nine 22 to 26-month-old female goats with a mean initial weight of 35 Kg (+/- 2.5 Kg). Four animals entered the study group and five the control group.

Each study group animal received a bone marrow biopsy of the iliac crest by a snarecoil bone marrow biopsy needle (*Ranfac Corp. Avon, MA, USA*). Bone marrow-derived mesenchymal stromal cells (MSC) were then isolated, cultured and expanded in a modified fibrin sealant substrate (*Evicel Ethicon Somerville NJ, USA*) [Figure 1] as follows: ten milliliters of bone marrow were aseptically collected into sterile heparinized tubes; according to previous reports for MSC isolation [1].The whole marrow washouts were layered onto Ficoll-Paque and centrifuged at 400g for 30 min at room temperature. Mononucleate cells ring was then removed, centrifuged and ammonium chloride solution was added in order to eliminate red blood cells. After that, cells were suspended in a specific medium (Dulbecco's modified Eagle Medium –DMEM – with

20% of fetal bovine serum with the addition of hepes), counted and seeded at 1.000.000/cm² .From 10 ml of bone marrow aspirate, we obtain a variable amount of MSC, ranging around 3-5.000.000 of cells. Cells were incubated at 37°C in humidified atmosphere with 5% CO₂.

To assess “stemness” of the isolated cells, cells were induced to transdifferentiate into adipocytes, osteoblasts and chondrocytes: In detail, 1-methyl-3-isobutylxanthine, dexamethasone, insulin and indometacin were used to induce adipogenic differentiation.

To promote chondrogenic differentiation cells were cultured without serum and with transforming growth factor beta, while osteogenic differentiation was obtained by adding dexamethasone, beta-glycerol phosphate and ascorbate.

The same procedure was performed in the control group with medium and fibrin sealant delivery without MSC.

2.3 Technique

Standard right upper lobectomy was performed on a goat model under general anesthesia without the need for single lung ventilation. Right lateral muscle-sparing thoracotomy was performed; mediastinal vessels for the upper lobe were isolated and then transected after double manual ligation. The right upper bronchus was then exposed, transected and clamped close to the tracheal take-off to avoid gas and oxygen leakage during intraoperative ventilation. Lobectomy was completed by fissure manual division similarly to human right upper fissureless lobectomy.

Bronchial stump closure was performed by single interrupted 3/0 polypropylene stitches (*Prolene Nonabsorbale Monofilament Ethicon Somerville NJ, USA*); the medial edge of the stump was left open and the caliber of the fistula homogenously created by a standard 4 millimeter caliber probe left inside the bronchial lumen at the time of last stitch application. Water submersion test under standard airway pressure of 15 cm H₂O was then performed to confirm the bronchial fistula and exclude other sites of air leakage.

Mean whole bronchial stump caliber was 10 mm (+/- 1mm) without any significant discrepancy among animals, the created fistula thus accounting for almost one third of the entire stump caliber. 24Ch (8.0 mm) silicone tubular drainage (*Kendall Argyle - Tyco Healthcare Tullamore, Ireland*) was placed and connected to a unidirectional Heimlich valve (*Laboratories Pharmaceutiques VYGON Ecoen, France*) before chest closure. The chest tube was routinely removed on post operative day 1.

On post operative day 7 cervical tracheostomy was performed under general anesthesia; a fiberoptic bronchoscope was inserted, the bronchial stump was inspected and the bronchial fistula identified. A transbronchial aspiration needle (*Olympus SmoothShot 19G x 13 mm*) was inserted through the bronchoscope operative channel; 5 ml of medium with modified fibrin glue (*Evicel Ethicon Somerville New Jersey, USA*) containing 2×10^6 /ml MSC were injected into the fistula and in the submucosal aspect of the bronchial stump. The same procedure was performed in the control group with medium and fibrin glue delivery without MSC.

On post operative day 28 all animals were euthanized by intravenous injection of pentobarbital sodium. Re-do ipsilateral thoracotomy was performed and the right tracheobronchial system was harvested and then frozen. Autoptic evaluation and pathology examination together with computed tomography and magnetic resonance imaging were also performed on the specimens.

2.4 “In vivo” experience

All animals receiving autologous MSC bronchoscopic transplantation presented BPF closure by extraluminal fibroblast proliferation and collagenous matrix development (**Figure 2**); none of them (0%) died during the study period. Both magnetic resonance and computed tomography imaging disclosed new peribronchial tissue occluding the bronchial stumps (**Figure 3a**). All control group animals still presented BPF after endoscopic treatment with fibrin sealant, and two of them (40%) died from pleural empyema. Magnetic resonance and computed tomography imaging (**Figure 3b**), as well as pathology examination (**Figure 4**) confirmed BPF persistence.

2.5 Comment

Bronchial stump dehiscence is still the most feared complication following curative lung resection [2]. For this reason the healing effects promoted by stromal cells – by transformation into mature cells with a specialized function or by enhancing intrinsic repair mechanisms - may represent an effective and only partially explored therapeutic option [3 - 4].

The mechanisms by which MSC induce tissue recovery are still widely debated, with cellular differentiation and paracrine effects being the two leading possibilities [5].

Our experimental model showed that extraluminal fibroblast proliferation and collagenous matrix development in the animals receiving MSC transplantation effectively occluded broncho-pleural fistula by tissue regeneration, thereby preventing almost always fatal pleural empyema. CT scan and MR imaging of specimens confirmed extrabronchial tissue proliferation in transplanted animals, suggesting peribronchial tissue regeneration as the stromal cell-induced reparative mechanism.

Clinical observation showed a clearly better outcome in the transplanted group, all animals being alive and without infection at the time of suppression. By contrast, two of the five control group animals died from pleural empyema, as disclosed at autopsy, thus confirming the clinical relevance of persistent BPF.

In conclusion, our data suggest that MSC targeted to BPF through submucosal bronchoscopic injection can promote tissue regeneration, thereby occluding bronchial stump dehiscence and preventing pleural empyema. Although these results provide a basis for the development of clinical therapeutic strategies, the exact mechanism by which they are obtained is not yet completely clear and further studies are required to understand exactly how stromal cells work in this field.

2.6 References

1. Pittenger MF, Mackay AM, Beck SC, et al. Multilineage potential of adult human mesenchymal stem cells. *Science*, 1999, 284:143-147
2. Gomez-de-Antonio D, Zurita M, Santos M, Salas I, Vaquero J, Varela A. Stem cells and bronchial stump healing. *J Thorac Cardiovasc Surg* 2010; 140: 1397-1401.
3. Wu Y, Chen L, Scott PG, Tredget EE. Mesenchymal stem cells enhance wound healing through differentiation and angiogenesis. *Stem Cells* 2007; 25: 2648-2659.
4. Mellough CB, Sernagor E, Moreno-Gimeno I, Steel DH, Lako M. Efficient stage-specific differentiation of human pluripotent stem cells toward retinal photoreceptor cells. *Stem Cells* 2012; 30: 673-686.
5. Fujimoto Y, Abematsu M, Falk A, Tsujimura K, Sanosaka T, Juliandi B, et al. Treatment of a mouse model of spinal cord injury by transplantation of human induced pluripotent stem cell-derived long-term self-renewing neuroepithelial-like stem cells. *Stem Cells* 2012; 30: 1163-1173.

2.7 Figure Legend

Figure 1: mesenchymal stem cells infected with a GFP(Green Fluorescent Protein) – expressing lentiviral vector, growing in a modified fibrin sealant substrate.

Figure 2: extraluminal fibroblast proliferation and collagenous matrix development by ematoxilin – eosin staining, observed at the distal part of the bronchial stump in transplanted animals.

Figure 3: computed tomography disclosed: **A)** peribronchial tissue occluding the bronchial stumps (white arrow); **B)** persistent broncho-pleural fistula (red arrow)

Figure 4: persistent broncho-pleural fistula in a control animal at pathology examination; note bronchial dehiscence close to non absorbable stitch and the typical tracheal takeoff of the right upper lobe of the goat.

Figure 5: gross image of the specimen demonstrating healing of the broncho-pleural fistula.

Figure 1: mesenchymal stem cells infected with a GFP(Green Fluorescent Protein) – expressing lentiviral vector, growing in a modified fibrin sealant substrate.

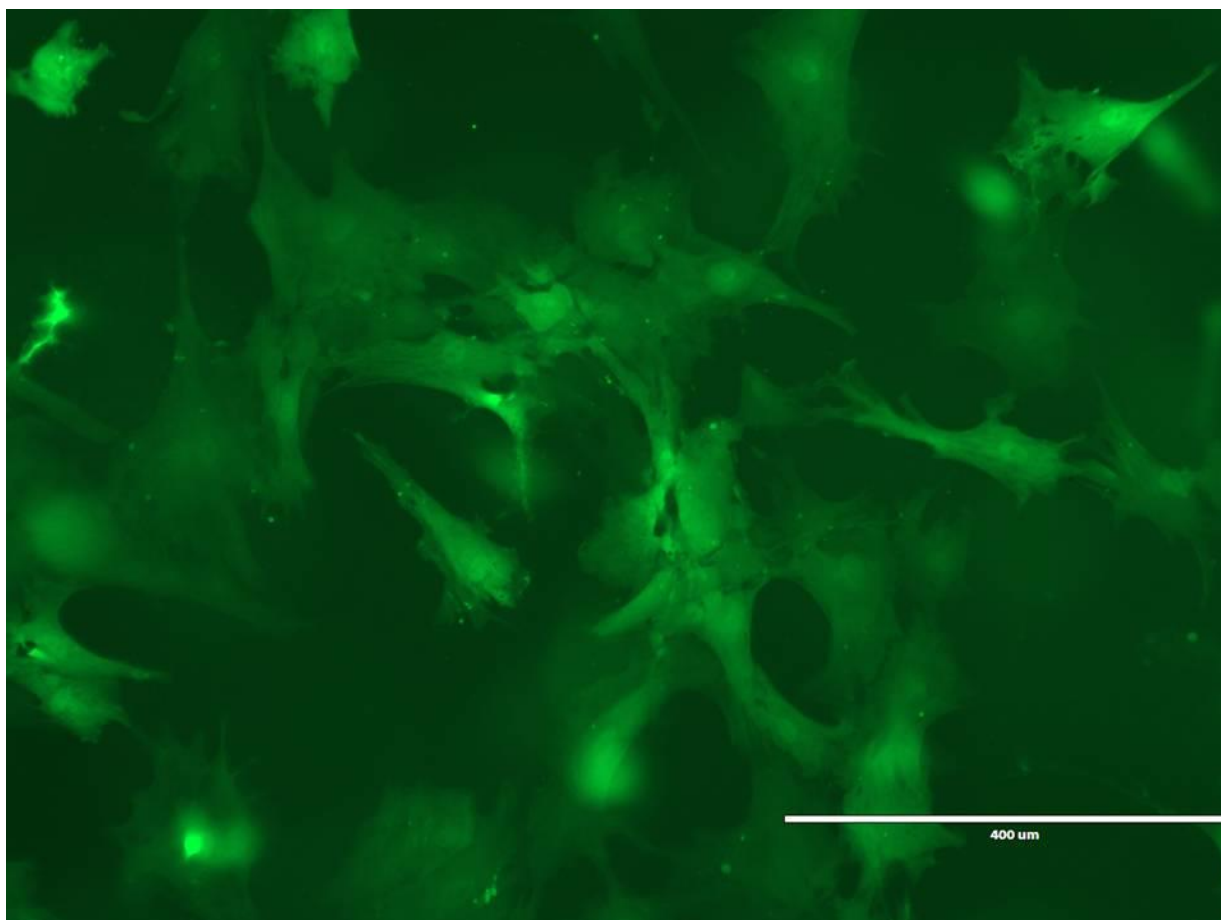


Figure 2: extraluminal fibroblast proliferation and collagenous matrix development by ematoxinilin – eosin staining, observed at the distal part of the bronchial stump in transplanted animals.

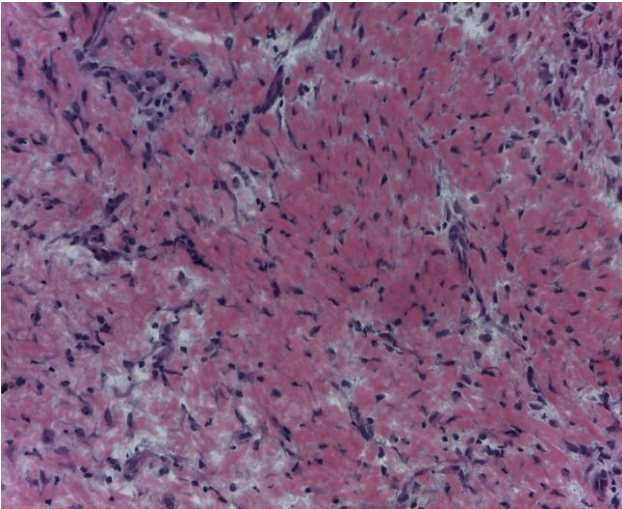


Figure 3: computed tomography disclosed: **A)** peribronchial tissue occluding the bronchial stumps (white arrow); **B)** persistent broncho-pleural fistula (red arrow)

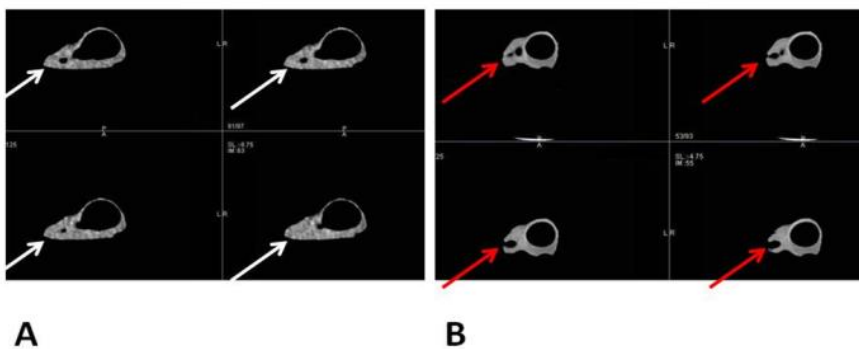


Figure 4: persistent broncho-pleural fistula in a control animal at pathology examination; note bronchial dehiscence close to non absorbable stitch and the typical tracheal takeoff of the right upper lobe of the goat.

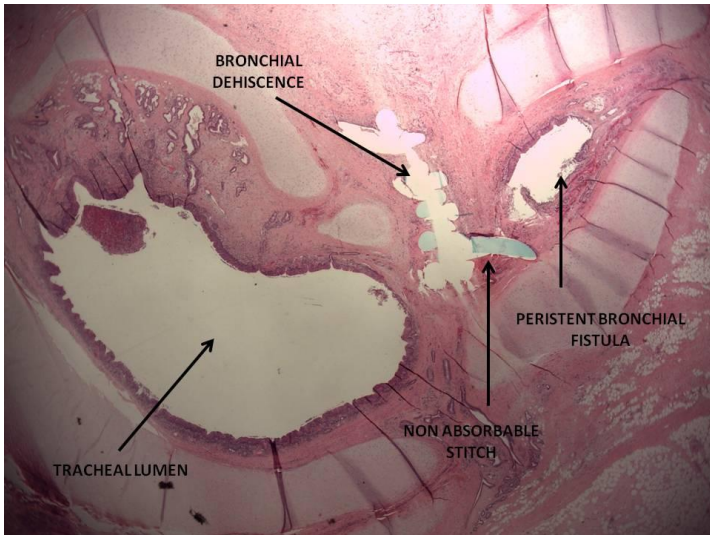
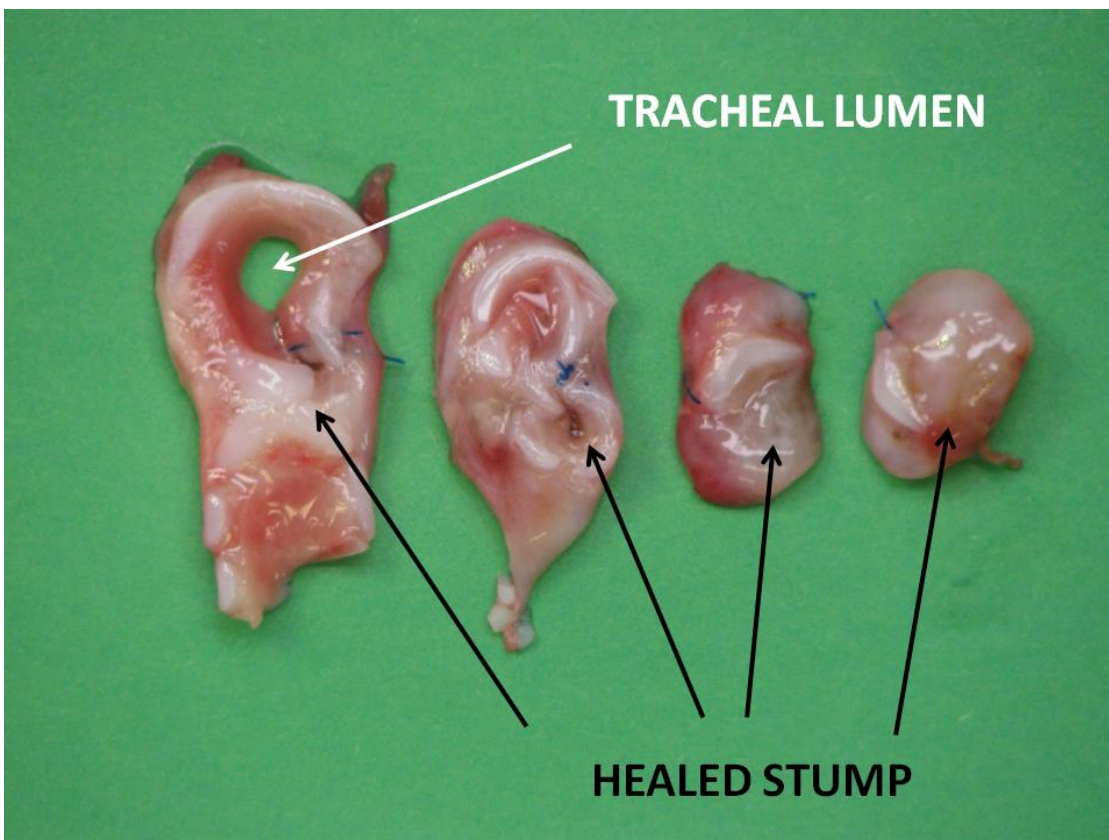


Figure 5: gross image of the specimen demonstrating healing of the broncho-pleural fistula.



3. CLINICAL AIRWAY RESTORATION: THE “FIRST-IN-HUMAN” EXPERIENCE

3.1 Abbreviation list

EPP: extrapleural pneumonectomy

FB: flexible bronchoscopy

AIFA: agenzia italiana del farmaco

BM: bone marrow

IRCCS: istituto di ricovero e cura a carattere scientifico

GMP: good manufacturing practice

TNC: total nucleated cells

PI: propidium iodide

PET: positron emission tomography

Encouraged by experimental bronchial wall restoration in large animals, and by functional human organ replacement elsewhere, we undertook autologous BMMSC bronchoscopic transplantation to treat a patient who developed BPF after right extrapleural pneumonectomy for malignant mesothelioma.

3.2 The recipient

A 42-year-old male firefighter presented with a diagnosis of clinical early-stage right malignant pleural epithelial mesothelioma. After videothoracoscopy and talc poudrage, the patient underwent three cycles of induction chemotherapy by cisplatinum and pemetrexed, followed by right extrapleural pneumonectomy (EPP).

The histology confirmed epithelial mesothelioma with macroscopic residual disease (R1) because of focal chest wall infiltration. The patient’s post-operative course was complicated by two episodes of

hemothorax, requiring redo thoracotomies for bleeding control. On post-operative day 18, the patient developed clinical symptoms related to BPF, confirmed by chest computed tomography (CT) **[Fig 1 A, Fig 2 A]** and flexible bronchoscopy (FB) **[Fig 2 A]**. Chest drainage was positioned and endopleural washings were started to reduce pleural cavity bacterial colonization, trying to prevent pleural empyema.

In the light of our successful preclinical work and to avoid an invasive and psychologically disabling open window thoracostomy we proposed to treat BPF by bronchoscopic transplantation of autologous bone marrow-derived mesenchymal stromal cells. In case of failure and the need for further treatment the proposed procedure would not have precluded salvage open window thoracostomy.

According to Italian legislation and following permission from the Ethics Committee of the European Institute of Oncology Milan and notification to the Italian drug agency (AIFA), written informed consent was obtained from the patient.

3.3 Bone marrow aspiration

The procedure was a standard bone marrow (BM) needle aspiration: the patient was positioned in prone decubitus; once a sterile site had been achieved in the area of the posterior iliac crest, lidocaine 2% (Xylocaina 20mg/ml AstraZeneca S.p.A. Basiglio - Milan, Italy) was infiltrated directly over the periosteum using a 22-gauge needle. A 16 gauge iliac aspiration needle (Monoject™ Illinois needle Covidien) was placed into the center of the posterior iliac prominence and carefully advanced through the cortical bone; 15 ml of BM were aspirated by a heparinized 20 ml syringe. The aspiration needle was then removed and pressure applied until bleeding ceased.

Soon after BM was directly transferred to the Cell Factory for MSC isolation and expansion.

3.4 Stromal cell isolation, expansion and culture

All the following procedures were performed at the Cell Factory of the IRCCS Foundation Ca' Granda Hospital, a hospital-based Good Manufacturing Practice (GMP) approved facility (authorization number 120/2007 of 05.07.2007 and subsequent confirmations, the last in 2012) for the production of cell therapy and tissue-engineered advanced medicinal products. The manipulations were performed under a class A biosafety cabinet in a class B GMP facility. Whole BM was directly seeded in alpha modified Eagle medium (Macopharma, Mouvaux, France) supplemented with 10% high quality gamma-irradiated fetal bovine serum (Gibco-Life Technologies, Carlsbad, CA, USA) at a concentration of 50,000 total nucleated cells (TNC) per cm² in a Cell Stack Chamber system (Corning, Lowell, MA, USA). After 72 hours, non-adherent cells were removed by washing with phosphate-buffered saline (Macopharma) and by completely changing the medium. The culture was monitored daily for colony appearance. On day 14, MSC at passage 0 were detached using 25 mL/layer of TrypLE- Select (Gibco) and subcultured in the same culture conditions at a concentration of 4,000 MSC /cm². The cell product was stopped at passage 1 when the cell target was reached [Fig 3]. All the cells for therapeutic use were cryopreserved: a cold solution containing 70% NaCl solution, 20% DMSO (Bioniche Lifesciences, Inc., Belleville, ON, USA), 10% human serum albumin (HSA, Kedrion, Lucca, Italy) was used. Immediately after addition of the cryopreservation solution, the bags (CryoMACS, Miltenyi Biotec, Bergisch Gladbach, Germany) were double sealed in their overwrap bag and cryopreserved using a controlled-rate freezer (Nicool Plus, Air Liquide, Paris, France) programmed to freeze at -1°C/ min until -110°C temperature. The frozen units were transferred and stored immediately to vapor-phase liquid nitrogen in dedicated tanks. The freezing curve was validated and recorded in the batch record.

3.5 MSC quality controls

On receipt of the BM the syringe was inspected and its integrity, correct identifications, and suitability of temperature during shipment were documented.

As requested by the GMP, the final product for clinical application is released according to defined acceptance criteria, which are relevant for evaluation of the cellular active principle. These specifications include: cell dose, purity (>80%), viability (>80%), sterility (no growth) endotoxins (< 0.25EU/mL), karyotype (normal 46,XX or 46,XY) and mycoplasma (no growth).

Before cell culture, TNC were counted by using a hematology analyzer (ABX MICROS 60, Horiba ABX, Irvine, CA, USA). Sterility testing of the starting material was performed in accordance with the European Pharmacopeia 2.6.27 using aerobic and anaerobic culture bottles (BaCT/ALERT BPN, BioMérieux Durham, NC, USA). During passages, cells were counted using an automated and validated method with an integrated fluorescence microscope (Nucleocounter®, Chemometec, Allerød, Denmark) allowing an accurate count of total viable cells excluding the nonviable cells by propidium iodide (PI). During cell harvesting and reseeded the culture product (1mL of cell culture supernatant before harvest) was tested for sterility as previously described. Before cryopreservation the final products were tested for all standard quality controls required for cell therapy products including sterility for microbial contamination (Ph. Eur.2.6.27), endotoxin (Ph. Eur. 2.6.14) and mycoplasma (Ph.Eur. 2.6.7). In addition, final products were also characterized in terms of cell dose, viability, purity and karyotype. The percentage of cells undergoing apoptosis and/or necrosis within the CD90+/CD45- cell compartment was quantitatively determined by Annexin V and PI staining (AnnexinV-FITC Apoptosis Detection kit, eBioscience, San Diego, CA, USA) as recommended by the manufacturer. Purity was determined by flow cytometry using antibodies against the classical MSC surface markers anti-CD90-FITC (Becton Dickinson, BD, San José, CA, USA), anti-CD105-PE (Beckman Coulter, Brea, CA, USA), anti-CD73-APC (Miltenyi Biotec) and against the hematopoietic marker

anti-CD45-PC7 (Beckman Coulter). Karyotyping was performed by conventional technique [13] on BMMSC collected by trypsinization. At least 20 metaphases were selected and analyzed.

Before administration, the cells (10×10^6) were thawed in normal saline solution containing 10% HSA and 12% ACD-A (Fresenius Kabi AG, Bad Homburg, Germany), washed and then resuspended in normal saline solution (5 mL final volume). The final product, contained in a sterily closed syringe, was shipped to the clinical department at controlled temperature (4-10°C) and injected within three hours from thawing.

3.6 Bronchoscopic implantation

Patient anesthesia was performed by propofol (Diprivan 10mg/ml AstraZeneca S.p.A. Basiglio, Milan, Italy) target-controlled infusion (TCI) 1.5 microg/ml and remifentanyl (Ultiva 1mg GlaxoSmithKline S.p.A., Verona, Italy) TCI 0.5 nanog/ml under Bispectral index (BIS) guidance to keep BIS as 65 +/- 5. No curarization was required and the procedure was conducted under spontaneous ventilation with nasopharyngeal tube endotracheal O₂ delivery at 4 L/min; electrocardiography (ECG), non-invasive blood pressure (NIBP), and O₂ peripheral saturation (sat O₂%) were monitored throughout the procedure. Vocal cord anesthesia was obtained by 4 ml lidocaine 2% (Xylocaina 20mg/ml AstraZeneca S.p.A. Basiglio - Milan, Italy) injected topically by the bronchoscope, before passing the vocal cords.

Flexible videobronchoscopy was performed by a 3.0 mm operative channel videobronchoscope (Olympus; Zoeterwoude, The Netherlands). The right main bronchus stump still presented a central 3 mm orifice accounting for about 30% of the stump length **[Fig. 2 A]**. Endoscopic water submersion test confirmed a small air passage through the orifice. Left bronchial system exploration did not disclose any relevant finding. Bronchoalveolar lavages were performed before starting stromal cell implantation.

Ten x 10⁶ autologous BMMSC were injected into the pars membranacea of the right main bronchus stump as close as possible to the orifice using a 19 gauge/13 mm long endoscopic needle (Olympus SmoothShot 19G _ 13 mm; Olympus; Zoeterwoude, The Netherlands).

Minor bleeding was observed in the injection sites, but it was self-limiting and did not require any treatment.

3.7 Postoperative care and monitoring

The postoperative course was uneventful: chest x ray and blood tests did not disclose any significant anomaly. The patient was discharged 24 hours after the procedure without any temperature and in good clinical conditions.

3.8 Clinical and bronchoscopic findings

The patient was followed up by weekly phone contact and clinical examination 30 days after the procedure; 60 days after implantation he underwent blood tests, chest CT scan, videobronchoscopy with bronchoalveolar lavage and biopsies.

Flexible bronchoscopy was performed under local anesthesia and spontaneous ventilation: endoscopic inspection of the right main bronchus stump disclosed a complete healing of the resection line and the central 3 mm orifice observed before BMMSC implantation was not longer visible **[Fig 2 A,B]**. Water submersion test did not disclose any air leakage; bronchoalveolar lavages and then bronchial biopsies were performed on the stump.

The left bronchial system did not disclose any significant finding; the procedure was uneventful and the patient was discharged 24 hours later in good clinical conditions.

3.9 Cytohistopathology

The specimen of bronchial mucosa obtained by bronchoscopic biopsy 60 days after stromal cell implantation showed a discrete coarctation induced by sample taking **[Fig. 4 A left lower box]**. However it was possible to appreciate a hyperplastic respiratory epithelium lying on a diffusely fibrotic lamina propria. Bands of smooth muscle fibers were reduced and replaced by fibroblasts **[Fig. 4 A]**.

The respiratory epithelium was composed of columnar cells without demonstrable cilia. We were not able to find goblet cells or neuroendocrine cells. The immunocytochemical stain for p40 - the DNp63 isoform considered highly specific for squamous/basal cell differentiation **[1]** - showed a well defined layer of basal cells and basal cell hyperplasia **[Fig 4 B]** consistent with repair.

3.10 Imaging

Pre-implant axial CT scan **[Fig 1 A]** showed patency of the lateral wall of the right bronchus and air bubbles within the right pleural effusion consistent with a diagnosis of BPF. This finding was confirmed by volume rendering of the airway **[Fig 1 C]** showing a subtle BPF (white circle) at the end of the right main bronchus, communicating with a small distal cavity.

Post-implant axial CT scan **[Fig 1 B]** showed closure of the BPF associated with disappearance of the air within the pleural effusion. Volume rendering of the airway **[Fig 1 D]** showed interruption of the fistula at its orifice from the right bronchus (white circle) where the BMMSC were injected.

Post-implant PET scan showed no uptake in the bronchial stump, and a moderate uptake on the internal surface of the chest wall.

3.11 Comment

Development of cell therapies and bioengineering approaches for lung diseases has rapidly progressed over the past decade [2]. A number of early reports initially suggested that bone marrow-derived cells, including MSC and other populations, could structurally engraft as mature differentiated airway and alveolar epithelial cells or as pulmonary vascular or interstitial cells [3]. Some recent reports continue to suggest that engraftment of the donor-derived airway can occur with several different types of bone marrow-derived cells [4].

MSC from bone marrow, adipose and placental tissue and other origins have been widely investigated for their immunomodulatory effects in a broad range of inflammatory and immune diseases [5]. However, the mechanisms of MSC actions are only partially understood. In addition to the paracrine actions of soluble peptide and other mediators, a growing body of data suggests that release of episomal or microsomal particles by MSC can influence the behavior of both surrounding structural and inflammatory cells [2]. A recent report suggests that MSC may also promote repair by activation of endogenous distal lung airway progenitor cell populations in mouse models [6]. Administration of MSC of either bone marrow or placental origin has also been demonstrated to decrease injury and inflammation in endotoxin or bacterially injured human lung explants [7].

MSC can also exert effects on lung inflammation and injury through primary interactions with the immune system rather than through direct actions in lung, in particular when the cells are systemically delivered [2]. Nonetheless, we decided to inject MSC topically into the fistula by bronchoscope rather than systemically by intravenous injection to avoid MSC dispersion to other areas involved by major inflammatory reactions, such as the thoracotomy site and pleural cavity, thus preventing MSC being sequestered by other competitive sites.

In the light of more recent findings, chronic persistent lung diseases with low level or smoldering inflammation – such as chronic obstructive pulmonary disease or idiopathic pulmonary fibrosis - may not

represent the best therapeutic targets for MSC intervention. On the contrary, more acute inflammatory lung or systemic diseases such as adult respiratory distress syndrome or sepsis/septic shock may be better targets [7]. Consequently, the scenario of an acute post-resectional BPF, where the acute inflammation component is prominent along with infection, may represent an ideal target for MSC clinical use in thoracic surgery.

Our first-in-human attempt to close BPF by this new minimally invasive approach was mainly boosted by the invasiveness of the only viable therapeutic alternative, namely open window thoracostomy. This procedure, based on chest wall opening by rib segment resection and requiring daily medication for a very long period, is very disabling and may present major healing problems in patients with chest wall residual neoplastic disease as in our case.

The use of autologous MSC eliminates the patient's need for lifelong immunosuppressant therapy and avoids the risk of infection. Bone marrow remains one of the best sites for MSC harvesting, although even adipose tissue is a viable option and may be further explored in the future. BMMSC isolation and culture, as well as quality controls, have yielded satisfactory results even in patients already submitted to induction chemotherapy.

Our patient's good clinical outcome may represent an interesting starting point for BMMSC application to the field of airway regeneration. However, several study limits must be emphasized and further analyzed by clinical and basic trials, before the reported technique can be considered an effective tool in daily clinical practice. Although the bronchoscopic view clearly shows an endoluminal complete bronchial restoration, we cannot exclude that an external healing process may have significantly contributed to BPF closure. Hence the clinical resolution of symptoms may be due in part to a physiological healing process rather than healing induced by bronchoscopic MSC transplantation. In addition, despite induction chemotherapy and two episodes of hemothorax following EPP, our 42-year-old patient was in very good clinical condition before receiving malignant mesothelioma treatments. In view of this, he may not be considered fully representative of our standard patient populations, usually much older and less fit when suffering from

post-resectional BPF. Lastly, the caliber of the BPF in our case accounted for about 30% of the stump length. It could be argued that a larger caliber fistula may not have benefitted from BMMSC transplantation because of the lack of a healthy bronchial scaffold in which to inject the cells.

There may be some concern that MSC may have an undesirable effect on tumor growth, but the in vivo evidence collected so far remains inconclusive. A recent clinical study in which autologous BMMSC from cancer patients were locally administered at the site of malignant primary bone tumor resection [8] showed no increase in the cancer local recurrence risk in patients treated with the cell-based therapy after an average follow-up of 15 years (10 – 20). Before treating our patient an accurate risk assessment was done, taking into consideration his preclinical and clinical experience and clinical situation. From the cell manufacturing standpoint, the production process and quality assessment were designed to preserve the safety of the final cell product and included in-depth cell growth evaluation, a short (one-passage) culture time and a complete karyotype assessment before releasing the product.

In conclusion, autologous BMMSC bronchoscopic transplantation in our patient proved safe and effective for closing post-resectional BPF following EPP for malignant mesothelioma, thereby avoiding an invasive end-stage salvage strategy like open window thoracostomy. This experience provides new evidence that clinical application of MSC may be further extended to restore post-resectional airway defects.

3.12 References

1. Bishop JA1, Teruya-Feldstein J, Westra WH, Pelosi G, Travis WD, Rekhtman N. p40 (Δ Np63) is superior to p63 for the diagnosis of pulmonary squamous cell carcinoma. *Mod Pathol*. 2012 Mar;25(3):405-15.
2. Weiss DJ. Current status of stem cells and regenerative medicine in lung biology and diseases. *Stem Cells* 2014;32:16-25.
3. Kassmer SH, Krause DS. Detection of bone marrow-derived lung epithelial cells. *Exp Hematol* 2010;38:564-573.
4. Wong AP, Keating A, Lu WY , Duchesneau P, Wang X, Sacher A, Hu J, Waddel TK. Identification of a bone marrow-derived epithelial-like population capable of repopulating injured mouse airway epithelium. *J Clin Inv* 2009;119:336-348.
5. Keating A. Mesenchymal stromal cells: New directions. *Cell Stem Cell* 2012;10:709-716.
6. Tropea KA, Leder E, Aslam M, Lau AN Raiser DM, Lee JH, Balasubramaniam V, Fredenburgh LE, Alex Mitsialis S, Kourembanas S, Kim CF. Bronchoalveolar stem cells increase after mesenchymal stromal cell treatment in a mouse model of bronchopulmonary dysplasia. *Am J Physiol Lung Cell Mol Physiol* 2012; 302:L829 – L837.
7. Lee JW Krasnodembskaya A, McKenna DH, Song Y, Abbott J, Matthay MA. Therapeutic effects of human mesenchymal stem cells in ex vivo human lungs injured with live bacteria .*Am J Respir Crit Care Med* 2013;187:751 -760.
8. Hernigou P, Flouzat Lachaniette CH, Delambre J, Chevallier N, Rouard H. Regenerative therapy with mesenchymal stem cells at the site of malignant primary bone tumour resection: what are the risks of early or late local recurrence? *Int Orthop*. 2014 Sep;38(9):1825-35.

3.13 Figure Legend

Figure 1: **A)** Axial CT scan before BMMSC injection shows patency of the lateral wall of the right bronchus, associated with air bubbles in a right pleural effusion, consistent with the diagnosis of BPF. **B)** Post-implant axial CT scan shows closure of the BPF, associated with disappearance of the air within the pleural effusion. **C)** Volume rendering of the airway shows a subtle BPF (white circle) at the end of the right main bronchus, communicating with a distal small cavity before BMMSC implantation. **D)** Post-implant volume rendering of the airway shows interruption of the fistula at its orifice from the right bronchus (white circle) where the BMMSC were injected

Figure 2: **A)** Flexible bronchoscopy view before BMMSC implantation disclosing the patency of the central part of the right bronchial stump, with a 3 mm orifice through which the titanium staple can be seen on the external aspect of the suture. **B)** Flexible bronchoscopy view 60 days after BMMSC implantation disclosing complete healing of the central bronchial dehiscence: the titanium staple is no longer visible on the external aspect of the suture.

Figure 3: Morphology of bone marrow mesenchymal stromal cells at passage 1.

Figure 4: **A)** Hyperplastic respiratory epithelium lying on a diffusely fibrotic lamina propria. Bands of smooth muscle fibers were reduced and replaced by fibroblasts. **B)** Immunocytochemical stain for p40 showing a well defined layer of basal cells and basal cell hyperplasia consistent with repair.

Figure 1: **A)** Axial CT scan before BMMSC injection shows patency of the lateral wall of the right bronchus, associated with air bubbles in a right pleural effusion, consistent with the diagnosis of BPF. **B)** Post-implant axial CT scan shows closure of the BPF, associated with disappearance of the air within the pleural effusion. **C)** Volume rendering of the airway shows a subtle BPF (white circle) at the end of the right main bronchus, communicating with a distal small cavity before BMMSC implantation. **D)** Post-implant volume rendering of the airway shows interruption of the fistula at its orifice from the right bronchus (white circle) where the BMMSC were injected

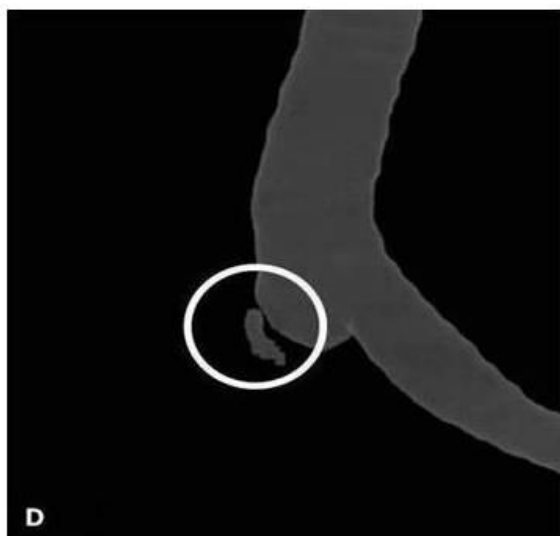
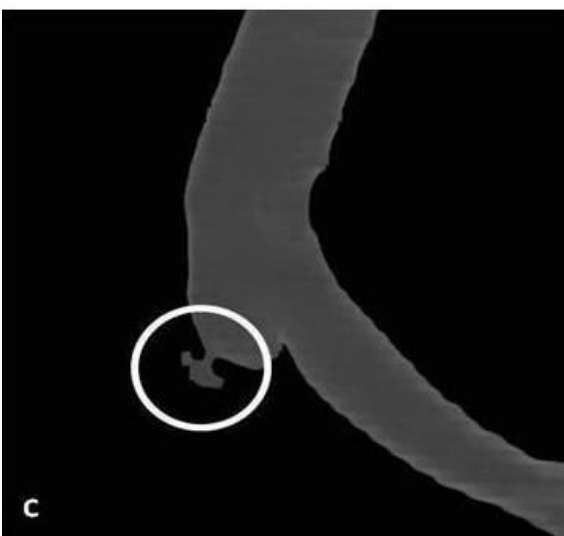
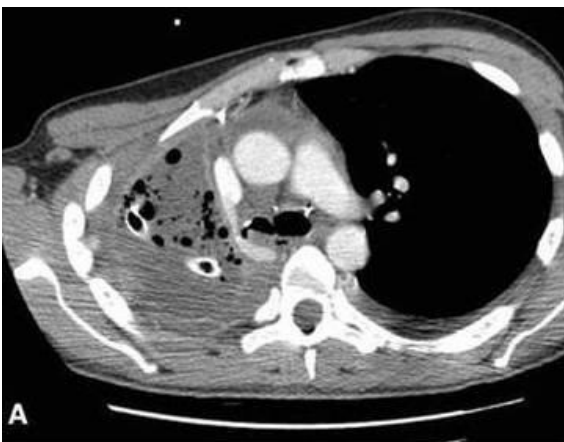
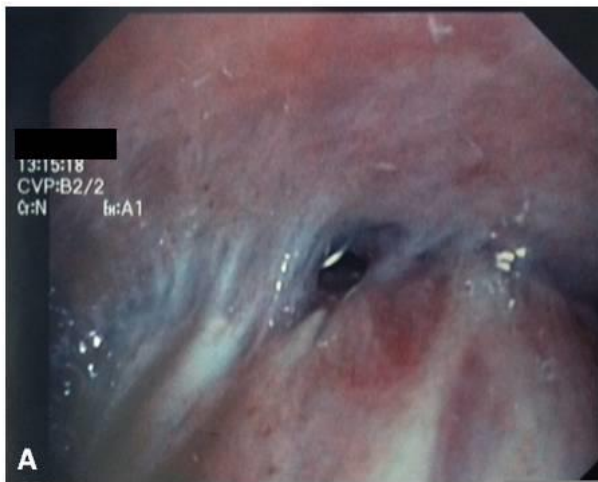
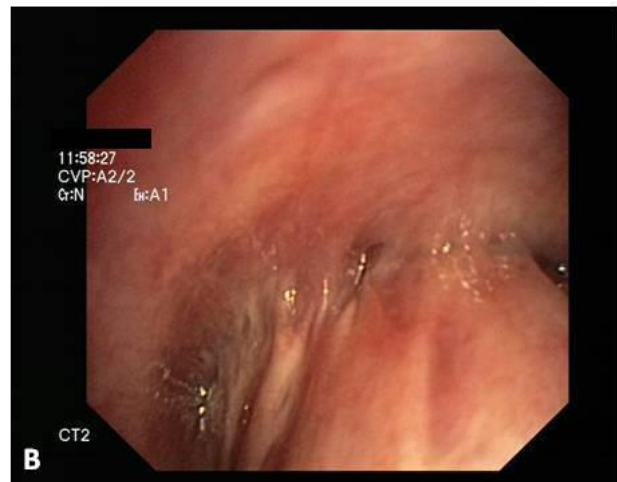


Figure 2: A) Flexible bronchoscopy view before BMMSC implantation disclosing the patency of the central part of the right bronchial stump, with a 3 mm orifice through which the titanium staple can be seen on the external aspect of the suture. **B)** Flexible bronchoscopy view 60 days after BMMSC implantation disclosing complete healing of the central bronchial dehiscence: the titanium staple is no longer visible on the external aspect of the suture.



PRE - IMPLANT



POST - IMPLANT

Figure 3: Morphology of bone marrow mesenchymal stromal cells at passage 1.

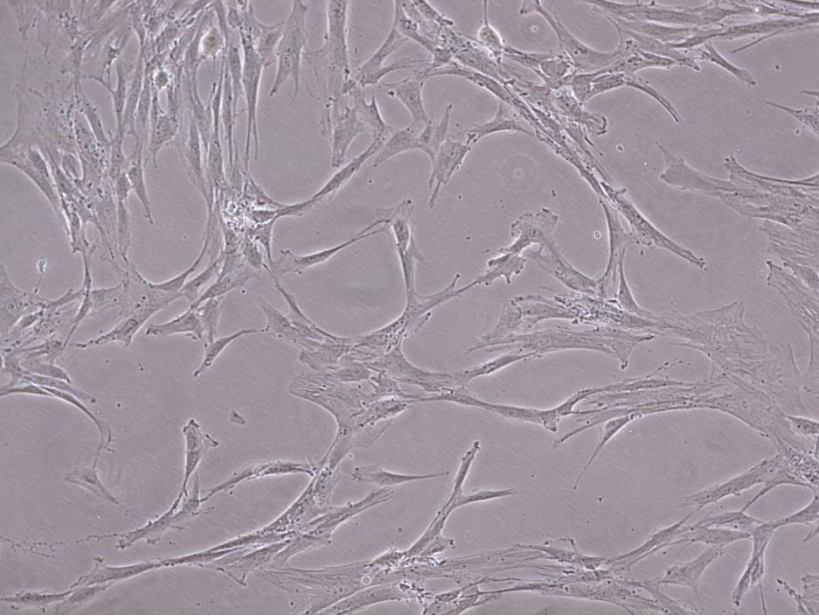
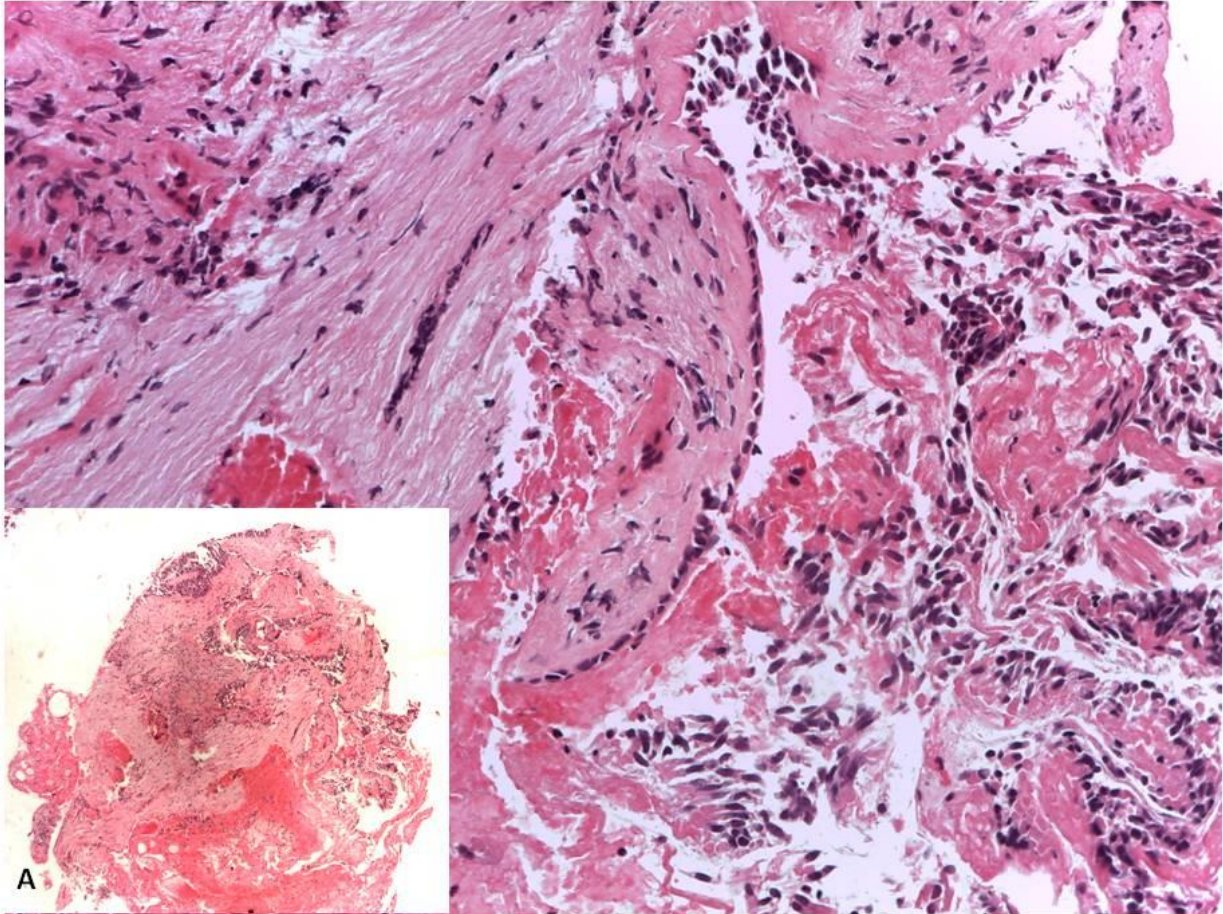


Figure 4: A) Hyperplastic respiratory epithelium lying on a diffusely fibrotic lamina propria. Bands of smooth muscle fibers were reduced and replaced by fibroblasts. **B)** Immunocytochemical stain for p40 showing a well defined layer of basal cells and basal cell hyperplasia consistent with repair.



4. “IN-VITRO” MSC TRACKING BY MAGNETIC RESONANCE IMAGING

4.1 Abbreviation list

PET: positron emission tomography

SPECT: single photon emission tomography

MRI: magnetic resonance imaging

18 FDG: 18 fluorodeoxyglucose

FDA: food and drugs administration

SPIO: superparamagnetic iron oxide

USPIO: ultrasmall superparamagnetic iron oxide

4.2 Introduction

Deficiencies in tissues and organs represent a huge challenge for medicine that has resulted in the emergence of regenerative medicine, which is an interdisciplinary field involving biology, medicine, and engineering aiming to repair, replace, maintain, or enhance tissue and organ functions by cell therapy [1].

Among the various stem cell populations used for cell therapy, adult mesenchymal stem cells (MSC) – also referred to as mesenchymal stromal cells – have emerged as a major new cell technology with a diverse spectrum of potential clinical applications [2].

Mesenchymal stromal cells (MSCs) are a population of undifferentiated multipotent adult cells that naturally reside within the human body and are generally defined as plastic-adherent, fibroblast-like cells possessing extensive self-renewal properties and potential to differentiate *in vivo* and *in vitro* into a variety of mesenchymal lineage cells [3].

MSC have the ability to migrate and engraft at sites of inflammation and injury in response to cytokines, chemokines and growth factors at a wound site. They can also exert local reparative effects through trans-differentiation into tissue-specific cell types or via the paracrine secretion of soluble factors with anti-inflammatory and wound-healing activities [4].

There is a need to specifically track these cells following transplantation in order to evaluate different method of implantation, to follow their migration within the body and to quantify their accumulation at the target [2].

Magnetic Resonance Imaging (MRI) has emerged as an excellent method for tracking cells both *in vivo* and *in vitro* [5]: many cell tracking studies have used iron oxide nanoparticle-based contrast agent to label cells for detection with MRI [6,7], while other studies have used perfluorocarbon nanoemulsion formulations [8-10]. Due to the absence of background signal, fluorine contrast agents, through a known reference phantom, are able not only to localize, but also to quantify the delivered cells by the direct quantification of the probe [11].

To date, however, no univocal results have been obtained and the best labelling method for MSC tracking by MRI need to be validated yet.

The purpose of this study was to assess if MSC can be labeled with super paramagnetic iron oxide (SPIO) nanoparticles as well as with perfluorocarbon (PFC) nanoemulsion formulations, without altering cell viability or differentiation, and to compare MRI data coming from iron- and fluorine-labelled MSC.

4.3 Materials and Methods

Rat mesenchymal stem cell culture

StemPro® Rat Alk Phos Expressing Mesenchymal Stem Cells (MSCs) were purchased from ThermoFisher Scientific (cat. N. R7789120) and cultured in α -Minimum Essential Medium, with nucleosides and GlutaMAX™ (ThermoFisher Scientific, cat. N. 32571), supplemented with 10% fetal bovine serum (ThermoFisher Scientific, cat. N. 10270) and 1% penicillin-streptomycin solution 100x (ECB3001D, Euroclone). MSCs were isolated from bone marrow of pooled transgenic Fischer 344 rats expressing the human placental alkaline phosphatase (hPAP) gene. MSCs viability, expression of cell surface markers and persistence of alkaline phosphatase expression was assessed by manufacturer. The medium was changed every third day and MSCs were maintained at 37°C, 5% CO₂.

SPIO labelling and ¹⁹F labelling

MSCs (passage 5) were treated with trypsin-EDTA (Euroclone, ECB3052D) and harvested by centrifugation at 300g for 5 minutes. Cells were counted by Trypan Blue (Thermo Scientific)

exclusion method to assess cell viability. A total of 6×10^6 cells were divided equally and plated in three tissue culture flask T75. A total of 2×10^6 MSCs were labeled with Molday ION Rhodamine-B (MIRB, BioPal Inc, Worcester, MA, USA), SPIO nanoparticles conjugated with Rhodamine B, that can be visualized by fluorescent imaging. MIRB has a colloidal size of 35 nm, a zeta potential of $\sim +31$ mV and an iron concentration of 2 mg/ml. MIRB was added to MSCs culture at the concentration of 50 $\mu\text{g/ml}$ in 6 ml culture medium for 24 hours at 37°C . A total of 2×10^6 MSCs were labeled with Cell Sense (CS-ATM DM Green), a PFC emulsion (30% vol./vol. of a perfluoro-15-crown-ether) conjugated with BODIPY dye, commercially obtained from Celsense Inc., Pittsburgh, PA, USA. Cell Sense has a total fluorine content of 120 mg/ml. MSCs were incubated with Cell Sense at the concentration of 10 mg/ml in 6 ml of culture media for 24 hours at 37°C . Unlabeled control (2×10^6 MSCs) was incubated in 6 ml of culture medium for 24 hours at 37°C . After incubation, the culture medium was aspirated and MSCs were washed twice with phosphate-buffered saline (PBS) to remove extracellular labeling agents. MSCs were harvested with trypsin-EDTA, centrifuged at 300g for 5 minutes and counted on hemacytometer with trypan blue exclusion method, for cell viability evaluation. A total of 10^4 labeled cells (MIRB-MSC and Cell Sense-MSC) were resuspended in culture medium and seeded on chamber slide. Culture medium was aspirated, cells were washed twice with PBS and fixed with paraformaldehyde (PFA) 4% for 15 minutes and stored at 4°C . Cells were permeabilized with PBS-Triton 0,1% for 10 minutes and nuclei were stained with DAPI (Thermo Fisher Scientific, D1306). Images were acquired via confocal microscopy (EZ-C1 scan-head equipped with Eclipse TE2000-E microscope; Nikon) using 20X (NA 0.85) objective and via z-scan 3D structured illumination microscopy (3D-SIM), using a 100X Apo-TIRF (NA 1.49) objective (Nikon). The percentage of labeled-MSCs was counted through ImageJ Software-Cell counter on five field for each slide.

Cell phantom preparation

Labeled MSCs were divided in four samples containing increasing concentrations of cells (0.125×10^6 , 0.25×10^6 , 0.5×10^6 , 1×10^6). MSCs samples were prepared by centrifugation at 300g for 5 minutes and each microcentrifugation tube was filled up with low-melting agarose 1% (Bio-Rad, 162-0017). Cell phantom of unlabeled cells and positive control with MIRB and Cell sense at the same concentration used for cell labeling were prepared.

MRI characteristics and features

The acquisitions were performed on a horizontal 7 T MRI scanner (Bruker BioSpec 70/30, Ettlingen, Germany) equipped with a gradient system reaching the maximum amplitude of 440 mT/m. Both MIRB labeled and CelSense labeled cells MRI and Magnetic Resonance Spectroscopy (MRS) were performed by a double nuclei ($^1\text{H} / ^{19}\text{F}$) volume resonator with an inner diameter of 72mm.

On MIRB labeled cells, MIRB phantom, and cells negative control T1 and T2 MRI maps were acquired with the same geometry (one 1mm coronal slice including the cells pellet). On MIRB phantom and cells negative control also T2* map was computed. T2 weighted images (T2-wi, TR = 3100ms, TE = 13ms) with 0.7mm slices in axial, sagittal, and coronal geometries were also acquired.

T1 mapping is based on a Rapid Acquisition with Relaxation Enhancement (RARE) sequence with Rare Factor of 2 and 28 images with a different repetition time TR (ranging from 25ms to 15000ms); echo time TE is set to 4.6ms. A Region of Interest (ROI) is then selected in correspondence of sample signal and its intensity plotted versus the image TR. The curve is fitted by the function

$$Y = A + C \left(1 - \exp - \frac{TR}{T_1} \right)$$

where A is the absolute bias and C the signal intensity.

T2 mapping is based on an a Multi Slice Multi Echo (MSME) sequence with a series of 200 echo-images with different TE (ranging from 5ms to 937.5ms); TR is set to 5000ms. A ROI is then selected in correspondence of sample signal and its intensity plotted versus the image TE. The curve is fitted by the function

$$Y = A + C \left(\exp - \frac{TE}{T_2} \right)$$

where A is the absolute bias and C the signal intensity.

T2* mapping is based on a Multiple Gradient Echo (MGE) sequence with a series of 500 echo images with different echo time (2ms – 807ms); TR is set to 5000ms. A ROI is then selected in correspondence of sample signal and its intensity plotted versus the image TE. The fitting is performed by the T2 maps analysis function.

All fitting are performed by OriginLab (Northampton, Massachusetts, USA) software.

On Cell sense labeled cells, Cell sense phantom, and cells negative control a ^{19}F non localized single pulse spectroscopy sequence (Flip angle = 90° , TR = 20s, 100 averages, acquisition time of 33

minutes) were acquired in order to ensure the visualization of each sample and, if visible, to quantify its ^{19}F atoms amount.

4.4 Results

SPIO and ^{19}F labelled cells viability and labelling efficiency

In order to investigate the cytotoxicity of iron oxide nanoparticles, the viability of cells was evaluated. The 86.8% of cells were viable and the percentage did not significantly differ from control group (89.8%). The percentage of labeled cells was 100%, assessed by fluorescence confocal microscope (fig 1).

After 24 hours of incubation with Cell Sense, 95% of MSCs were labeled with the perfluorocarbon tracer and there was a slight decrease in cell viability, compared to control (83.6% vs 89.8%). Labeled tracer was found in vesicles diffusely distributed in MSCs cytoplasm (fig 1).

SPIO labelled imaging

MIRB shows the following relaxation parameters: $T_1 = 559\text{ms}$, $T_2 = 13.4\text{ms}$, $T_2^* = 3.6\text{ms}$. Not labeled cells T_1 , T_2 , and T_2^* values are 2041ms, 132ms, 4.6ms respectively. In Table 1, T_1 and T_2 values of MIRB labeled cells are reported.

T_2w images show a hypointense signal corresponding to labeled cell pellet regions, which are visible in all the samples with different number of cells (Figure 2).

^{19}F labelled imaging

Only pellets containing 1 million and half a million of Cell sense labeled cells show a detectable signal, although having a very low intensity in comparison with noise (Figure 3). While negative control cells do not show any signal, the Cell sense phantom show its characteristic ^{19}F peak.

4.5 Discussion

Stem cells are being intensively studied for infusion or transplantation into tissue for purposes of repair, revascularization, and other therapeutic measures [12-14]. The serial visualization and tracking of transplanted stem cells, including the assessment of their presence at the site of the injury, and their migration or retention in other sites, are still issues to be resolved before many pre-clinical studies can be turned into clinical studies. Indeed, there is still some uncertainty on the

safety of the use of stem cells [15] and further pre-clinical validation is necessary before their use may be transferred into clinical applications.

A safe, noninvasive, and repeatable imaging modality, able to track the injected stem cells in vivo would be able to solve some of the current issues, but to date, no individual imaging modality can be considered a one-stop shop for monitoring therapies based on the use of stem cells. Therefore, the choice of modality for labeling and in vivo tracking of stem cells depends on the questions being addressed.

Thanks to its non invasivity and high spatial resolution (ranging from 50 μ m in animals and up to 300 μ m in whole body clinical scanners), MR imaging is a popular choice for in vivo cell tracking in preclinical and clinical studies [16]. To be tracked using MRI, stem cells need to be enriched with a contrast agent that produces a sufficient positive or negative signal enhancement to distinguish them from the image background. Contrast agents containing SPIO nanoparticles have been the preferred agent for short-term stem cell tracking, due to the pronounced signal change that even small amounts of these contrast media can create (owing to the so called “blooming artifact”).

In this study, taking this ‘negative’ contrast effect, we were able to detect by a high field MR, even a small number of MIRB labelled cells (0.125×10^6).

This specific feature of SPIO, that allows the detection of even very small numbers of labeled cells, may vary depending on the anatomical structure under evaluation, and can be confounded with other sources of magnetic susceptibility differences, such as bleedings, blood vessels or air.

Considering that future pre-clinical applications may include evaluation of the lungs, as by using MSCs in repair processes, such as broncho-pleural fistulas [17], as for assessing their migration into the lungs, we decided to try the labelling of MSCs also with perfluorocarbon (PFC) nano-emulsions, which can be detected with ^{19}F MRI [8,9]. The ^{19}F nucleus is particularly suitable for labeling as its relative MR sensitivity is only 17% less than that of ^1H [18]. Since the level of background ^{19}F signal in host tissue is virtually absent, overlaying the ^{19}F image on an anatomical usual image (such as a T2 or T1 weighted image) would allow a quantitative tracking of labeled cells in vivo.

In this study, we were able to label MSCs by a PFC emulsion conjugated with BODIPY dye with a slight decrease in cellular viability, compared to control (83.6% vs 89.8%), but only pellets containing 1×10^6 and 0.5×10^6 of Cell sense labeled cells show a detectable signal.

Compared to labeling and tracking with metal-based contrast agents ^{19}F labeling is less sensitive, therefore a relatively large amount of ^{19}F , or a large number of labeled cells must accumulate in order to generate sufficient signal-to-noise ratio (SNR) for tracking.

Our data support the use of both types of contrast media (SPIO and PFC) for labelling of MSCs, although further efforts should be dedicated to get an improvement in efficiency of PFC labelling.

4.6 Acknowledgements

The authors wish to thank Cellsense Inc. and the person of Dr. Charles O'Hanlon for supply of Cellsense CS-1000 ATM green.

4.7 References

1. Dai R, Wang Z, Samanipour R, Koo KI, Kim K Adipose-Derived Stem Cells for Tissue Engineering and Regenerative Medicine Applications Stem Cells Int. 2016;2016:6737345.
2. Ribot EJ, Gaudet JM, Chen Y, Gilbert KM, Foster PJ In vivo MR detection of fluorine-labeled human MSC using the bSSFP sequence Int J Nanomedicine. 2014 Apr 8;9:1731-9.
3. Pittenger MF, Mackay AM, Beck SC, Jaiswal RK, Douglas R, Mosca JD, Moorman MA, Simonetti DW, Craig S, Marshak DR Multilineage potential of adult human mesenchymal stem cells Science. 1999 Apr 2;284(5411):143-7
4. Petrella F, Rizzo S, Borri A, Casiraghi M, Spaggiari L Current Perspectives in Mesenchymal Stromal Cell Therapies for Airway Tissue Defects Stem Cells Int. 2015;2015:746392
5. Helfer BM, Balducci A, Sadeghi Z, O'Hanlon C, Hijaz A, Flask CA, Wesa A ^{19}F MRI tracer preserves in vitro and in vivo properties of hematopoietic stem cells Cell Transplant. 2013;22(1):87-97.
6. Heyn C, Bowen CV, Rutt BK, Foster PJ Detection threshold of single SPIO-labeled cells with FIESTA Magn Reson Med. 2005 Feb;53(2):312-20

7. Stuckey DJ, Carr CA, Martin-Rendon E, Tyler DJ, Willmott C, Cassidy PJ, Hale SJ, Schneider JE, Tatton L, Harding SE, Radda GK, Watt S, Clarke K Iron particles for noninvasive monitoring of bone marrow stromal cell engraftment into, and isolation of viable engrafted donor cells from, the heart Stem Cells. 2006 Aug;24(8):1968-75.
8. Bonetto F, Srinivas M, Heerschap A, Mailliard R, Ahrens ET, Figdor CG, de Vries IJ A novel (19)F agent for detection and quantification of human dendritic cells using magnetic resonance imaging Int J Cancer. 2011 Jul 15;129(2):365-73.
9. Krafft MP Fluorocarbons and fluorinated amphiphiles in drug delivery and biomedical research Adv Drug Deliv Rev. 2001 Apr 25;47(2-3):209-28.
10. Ahrens, E. T., Helfer, B. M., O'Hanlon, C. F., & Schirda, C. Clinical cell therapy imaging using a perfluorocarbon tracer and fluorine-19 MRI. (2014). Magnetic Resonance in Medicine, 72(6), 1696-1701].
11. Tirota I, Mastropietro A, Cordiglieri C, Gazzera L, Baggi F, Baselli G, Bruzzone MG, Zucca I, Cavallo G, Terraneo G, Baldelli Bombelli F, Metrangolo P, Resnati G. A superfluorinated molecular probe for highly sensitive in vivo(19)F-MRI. J Am Chem Soc. 2014 Jun 18;136(24):8524-7. doi: 10.1021/ja503270n.
12. McKay R. Stem cells: hype and hope. Nature 2000; 406:361–364
13. Deans RJ, Moseley AB. Mesenchymal stem cells: biology and potential clinical uses. Exp Hematol 2000; 28:875–884.
14. Kolios G, Moodley Y. Introduction to stem cells and regenerative medicine. Respiration. 2013;85(1):3-10.
15. Blum B, Benvenisty N. The tumorigenicity of diploid and aneuploid human pluripotent stem cells. Cell Cycle. 2009 Dec;8(23):3822-30.
16. Tong L, Zhao H, He Z, Li Z. Current Perspectives on Molecular Imaging for Tracking Stem Cell Therapy DOI: 10.5772/53028
17. Petrella F, Toffalorio F, Brizzola S, De Pas TM, Rizzo S, Barberis M, Pelicci P, Spaggiari L, Acocella F. Stem Cell Transplantation Effectively Occludes Broncho-pleural Fistula in an Animal Model. Ann Thorac Surg. 2013 Dec 23. pii: S0003-4975(13)02346

18. Kok MB, de Vries A, Abdurrachim D, Prompers JJ, Gröll H, Nicolay K, Strijkers GJ. Quantitative ^1H MRI, ^{19}F MRI, and ^{19}F MRS of cell-internalized perfluorocarbon paramagnetic nanoparticles. *Contrast Media Mol Imaging*. 2011 Jan-Feb;6(1):19-27. doi: 10.1002/cmml.398.

4.8 Tables and Figures Legends

Table 1. MIRB labeled cells relaxometry results

Figure 1: Cell Sense-labeled MSC and MIRB-labeled MSC. Fluorescence images of MSCs labeled with Cell Sense (A and C) or MIRB (B and D). Images were acquired by confocal microscopy (A and B) and 3D-SIM super resolution microscopy (C and D). Scale bar A and B: $50\mu\text{m}$, scale bar C and D: $2\mu\text{m}$.

Figure 2: A) Coronal and axial T2-wi of six sample containing no-labelled cells (1), MIRB (2), and different amounts of MIRB labeled cells (3, 4, 5, 6). B) T2 data fitting of the 1×10^6 cells pellet. C) T2 decays of the labeled cells samples.

Figure 3: ^{19}F MRS of five samples containing Cell sense (1) and different amounts of Cell sense labeled cells: 1 million (2), 5×10^5 (3), 2.5×10^5 (4), 1.25×10^5 (5). Black arrows highlight Cell sense ^{19}F peak. The wide peak at -5ppm is due to the resonator coil itself

Figure 1: CellSense-labeled MSC and MIRB-labeled MSC. Fluorescence images of MSC labeled with CellSense (green) or MIRB (red). Images were acquired by confocal microscopy (A and B) and structured illumination microscopy (C and D). Scale bar: 2μm

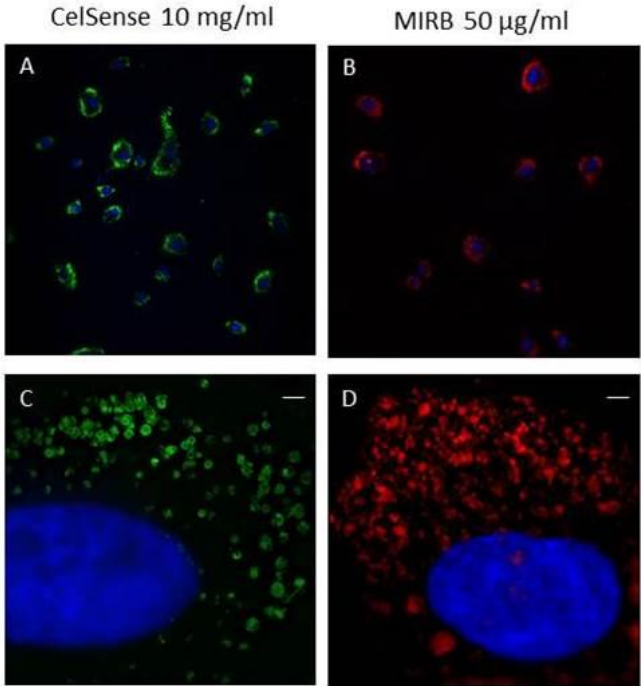


Figure 2: A) Coronal and axial T2-wi of six sample containing no-labelled cells (1), MIRB (2), and different amounts of MIRB labeled cells (3, 4, 5, 6). B) T2 data fitting of the 1x10⁶ cells pellet. C) T2 decays of the labeled cells samples.

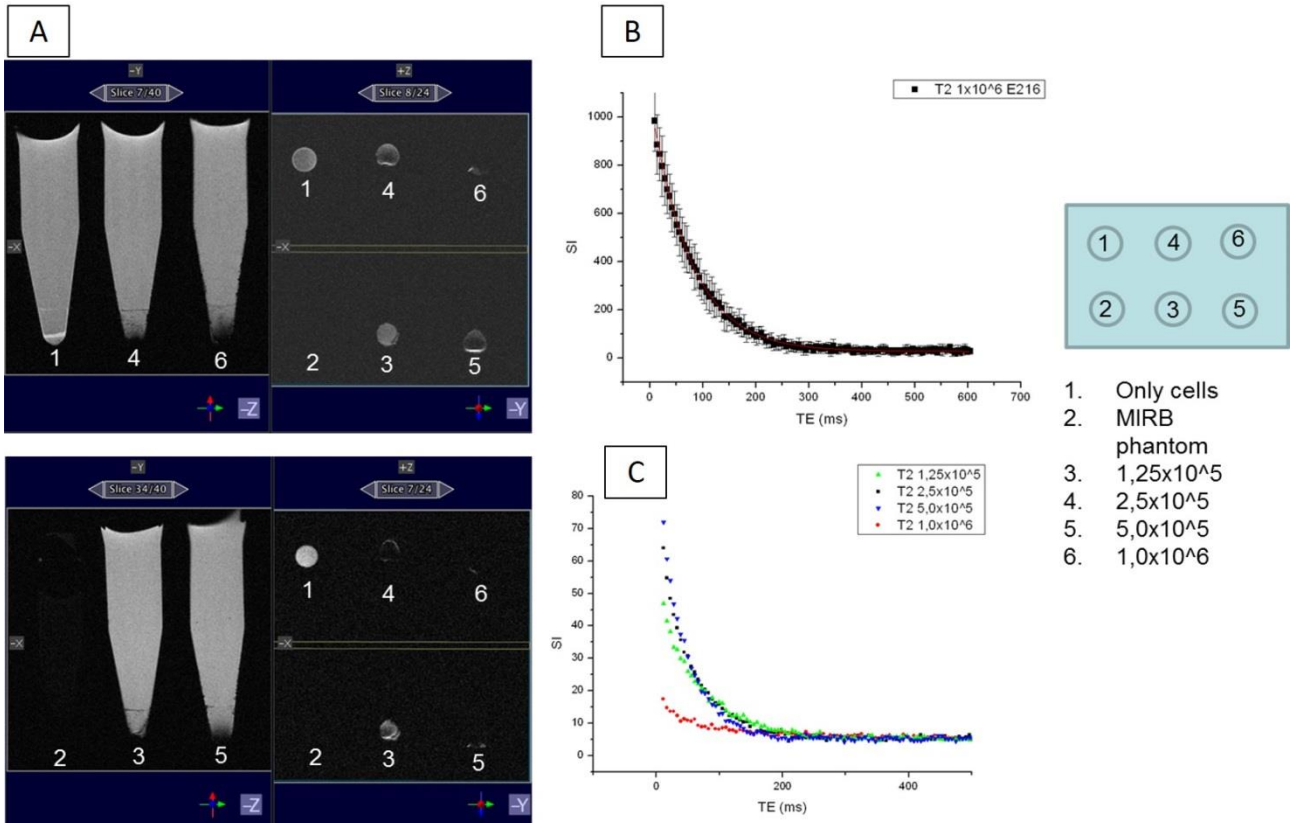
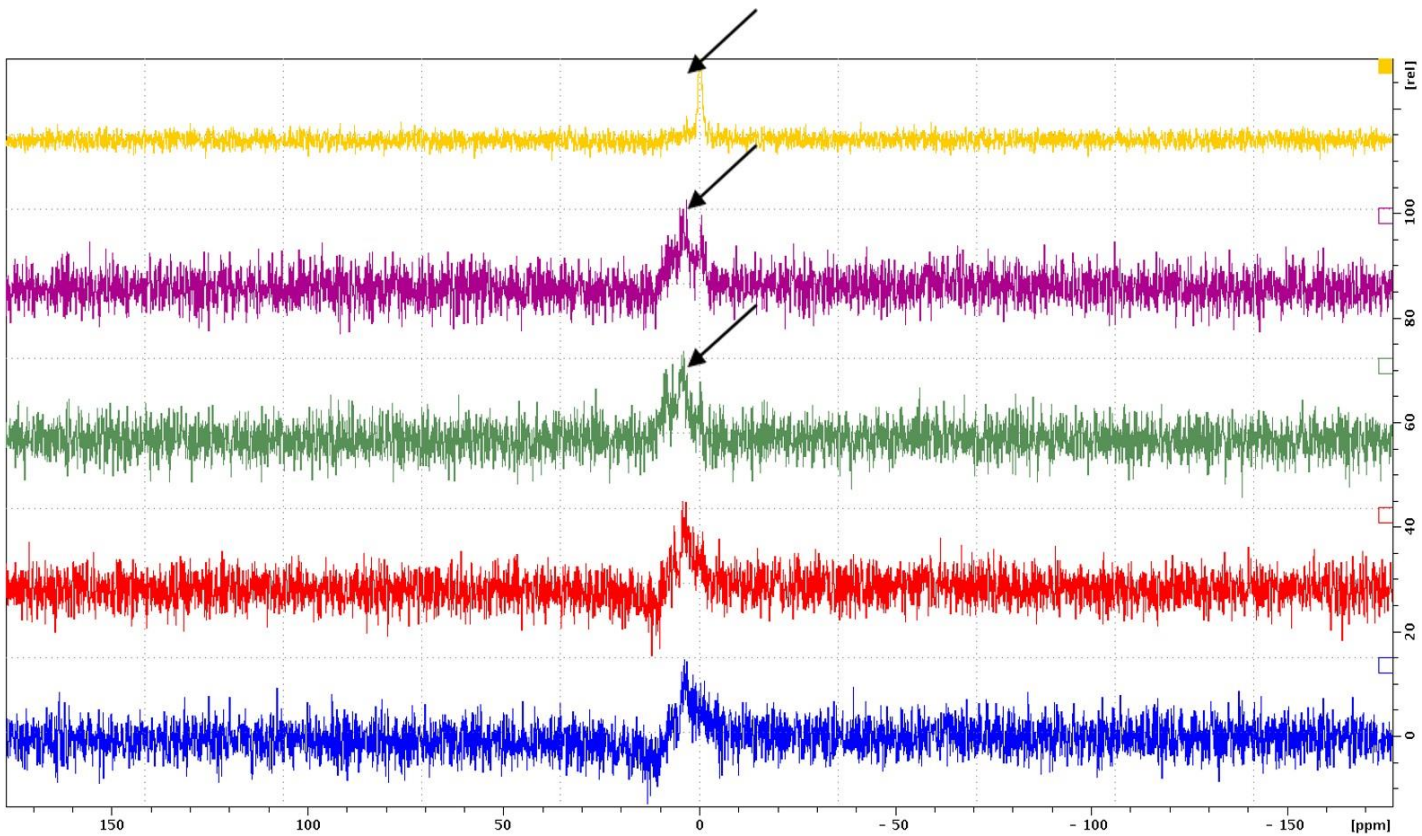


Figure 3: ^{19}F MRS of five samples containing Cell sense (1) and different amounts of Cell sense labeled cells: 1 million (2), 5×10^5 (3), 2.5×10^5 (4), 1.25×10^5 (5). Black arrows highlight Cell sense ^{19}F peak. The wide peak at -5ppm is due to the resonator coil itself



5. FUTURE PERSPECTIVES: ADIPOSE DERIVED MESENCHYMAL STROMAL CELLS AND GRANULOCYTE-COLONY STIMULATING FACTOR FOR AIRWAY TISSUE DEFECTS

5.1 Abbreviation List

G-CSF: granulocyte-colony stimulating factors

AMSC: adipose mesenchymal stromal cell

IFN γ : interferon-gamma

IDO: indoleamine 2,3-dioxygenase

HLA: human leukocyte antigen

5.2 Clinical background

We have previously demonstrated the feasibility, the efficacy and safety of BPF closure by bronchoscopic injection of autologous bone marrow–derived mesenchymal stromal cells (BMMSC), both in preclinical and clinical settings. However this procedure is time-consuming thus being very often inapplicable to patients in life-threatening condition which cannot wait for longer than few days. We are now developing a “fast-track” technique of BPF closure by autologous adipose derived mesenchymal stromal cells (AMSC) bronchoscopic injection together with systemic administration of granulocyte colony-stimulating factor (G-CSF) that is a well-known cytokine presenting regenerative properties both by bone marrow stromal cells mobilization, both by a direct trophic effects on the damaged tissues.

Mesenchymal stromal cells are considered a promising tool for cell therapy in regenerative medicine, being able to restore damaged tissue by their complex “cross-talk” interaction with the local environment; G-CSF is a well-known cytokine whose clinical effect may be mediated through bone marrow cell (BMC) mobilization, typically induced by G-CSF. Mobilized stromal cells might be responsible for the regeneration

of damaged tissues and organs. Alternatively or additionally, G-CSF may have a direct trophic effect, also suggested by the fact that various tissues have been shown to express high levels of G-CSF receptor.

The hypothesis of our study is to treat BPF by local MSC bronchoscopic injection together with systemic G-CSF iv administration, restoring damaged tissue and promoting bronchial dehiscence healing.

5.3 Preliminary data

Adult mesenchymal stromal cells (MSCs), including adipose-derived mesenchymal stromal cells (ASCs) are considered a promising tool for cell therapy in regenerative medicine or for treating inflammatory and autoimmune diseases due to their immunomodulatory capacity and paracrine effects through trophic factors with antifibrotic, antiapoptotic, or pro-angiogenic properties [1]

ASCs show immunomodulating properties and regulate the function of a broad variety of immune cells including B lymphocytes, T lymphocytes, NK cells, monocyte-derived dendritic cells, and neutrophils [2]. The specific molecular and cellular mechanisms rely on both cell contact-dependent mechanisms and paracrine effects through the release of various soluble factors including hepatocyte growth factor, prostaglandin-E2, transforming growth factor- β 1, indoleamine 2,3-dioxygenase (IDO), nitric oxide, interleukin (IL)-10, IL-6, heme oxygenase-1, or human leukocyte antigen (HLA)-G5 [14]. Among these factors, IDO activity appears to be a key player in human ASC-mediated immunomodulation [3]. ASCs have to be primed by inflammatory mediators, including interferon-gamma (IFN γ), IL1 β , and tumor necrosis factor alpha (TNF) alpha which are strongly secreted by activated immune cells in inflamed environments (i.e., the perianal fistulas) in order to show their full immunomodulatory properties [4]

In addition to the immunomodulatory properties, ASCs are considered immune privileged because: (1) they constitutively express only low levels of cell-surface HLA class I molecules and lack expression of HLA class II, CD40, CD80, and CD86; (2) after stimulation of ASCs by inflammatory mediators, there is up regulation of HLA class I and induced expression of HLA class II molecules on the ASCs, but without the expression of

classic costimulatory molecules which would lead to anergy of T lymphocytes and immune tolerance; and (3) upon stimulation with inflammatory mediators released by activated immune cells, ASCs trigger an anti-inflammatory and immunomodulatory response (mainly through the induction of IDO) that may also modulate the immune recognition. These factors may contribute to a delayed or reduced activation of the innate and adaptive immune responses against allogeneic ASCs by the recipient's immune system. This immune privilege of ASCs therefore supports the feasibility even of allogeneic other than autologous treatments without the requirement of suppression of host immunity [5,6]. The therapeutic benefit of human ASCs has been reported in a number of experimental models of inflammatory diseases including inflammatory bowel disease [7,8]. In humans, local administration of autologous ASCs and bone-marrow mesenchymal stromal cells has been used to treat perianal fistulas with promising results from a safety and efficacy perspective [9–12].

Granulocyte colony-stimulating factor (G-CSF) is a well-known cytokine shown to have a regulatory effect on haematopoiesis, and it is widely employed in onco-haematology to reduce chemotherapy-induced haematopoietic toxicity [13]. Moreover, several recent reports suggest a possible benefit from G-CSF administration in various diseases, including liver failure, cardiac ischemia and certain diseases with neurological and vascular damage [14]. In these clinical settings, the possible therapeutic effect of G-CSF may be mediated through bone marrow cell (BMC) mobilization, typically induced by G-CSF. Mobilized stromal cells might be responsible for the regeneration of damaged tissues and organs. Alternatively or additionally, G-CSF may have a direct trophic effect, also suggested by the fact that various tissues have been shown to express high levels of G-CSF receptor [15]. The use of G-CSF in non-haematological disease is also favoured by the high tolerability and ease of use of this cytokine. Among non-haematological tissues, G-CSF has been proposed to improve skeletal tissue repair processes. Several other functions have been attributed to G-CSF, including the modulation of the inflammatory pathway and an anti-apoptotic as well as a direct trophic effect [16]. Taken together, these activities suggest that G-CSF may have a role in repairing tissues defects and therefore may be suitable for use in treatment programs aimed at accelerating tissue repair.

5.4 Experimental design aim 1

Patients with clinical diagnosis of post resectional bronchial fistula will be admitted, mostly as emergency admission. They will be then clinically stabilized and submitted to fiberoptic bronchoscopy and chest computed tomography and routine lab exams.

When BPF is confirmed, the patient will receive at least 24 Ch chest tube insertion on the side of the fistula – that represents the standard acute treatment in order to avoid iperthensive pneumothorax and mediastinal shift; subsequently the patient will be transferred to operative room where he will receive 100 ml abdominal lipoaspiration **[Figure 1]**. This aspirate will be then centrifugated (2500 rotations x 2 minutes) and 5 ml of lipoaspirate will be injected into the fistula through a Wang bronchial needle inserted by a flexible bronchoscope, under sedation but without curarization and under spontaneous breathing. 5 ml of fibrin glue is then bronchoscopically delivered upon the graft, to fix the implant within the bronchial stump, to avoid MSC scattering by coughing or breathing; we have previously demonstrated that MSC easily survive and remain active within fibrin glue **[17]**; subsequently iv G-CSF will be given at 10 micrograms/kilogram/day for three consecutive days.

5.5 Experimental design aim 2

The patients will be treated by the supposed minimum effective dose (based on our previous experimental and clinical experience) of 1×10^6 MSC **[17,18]**. If closure of the fistula is incomplete at bronchoscopic check at day 7, the same treatment is repeated at the same dose on postoperative day 8 (total amount of cell: 2×10^6 MSC); in case of further treatment needing, the last administration of MSC is done at post op day 16 (total amount of cell 3×10^6 MSC); if the third treatment is not effective yet, standard surgical treatment is indicated (debridement, thoracosotomy or other surgical treatment).

Daily blood test, chest x rays and physical examination as well as weekly bronchoscopic check are performed in order to early disclose potentially adverse events.

5.6 Experimental design aim 3

Daily chest x rays and physical examination as well as weekly bronchoscopic check are performed to check the procedure results; post treatment CT scan is performed in case of supposed successful treatment to confirm bronchial stump healing; 30 and 60 days follow up by chest x ray and inspective flexible bronchoscopy are performed to confirm the long term efficacy of the procedure

5.7 Methodologies and statistical analyses

We plan to enroll 12 patients in the 3-year period, with a median recruitment of 4 patients/year. Complete bronchial dehiscence as well as poor clinical conditions will be considered as contraindications to the proposed treatment and patients will be treated according to standard approaches.

Patient fulfilling the enrollment criteria, will be given a detailed informed consent to acquaint themselves on the proposed procedure; rescue surgical invasive procedure (open window thoracostomy) will be proposed in case of failure of the minimally invasive stromal cell based technique, after the third session or - if needed – earlier.

This is a single arm, prospective study; no randomization is then needed and the techniques efficacy, as well as potential adverse events, are evaluated by comparison with literature data of standard techniques, both in terms of bronchial fistula healing as well as morbidity and mortality.

5.8 Expected outcomes

We expect to acquire data on types and locations of fistulas mainly benefitting from the proposed treatment, probably small caliber fistulas or fistulas following lobectomy rather than pneumonectomy, left and upper lobar sided; we expect to have information about the minimum effective dose in terms of MSC delivery as well as of number of treatments and days needed for clinical bronchial healing.

5.9 Risk analysis, possible problems and solutions

In recent decades, there has been tremendous hope that stromal-cell–based technologies would introduce a new era of regenerative medicine, revolutionizing the treatment of disease. These hopes have been stoked by reports that often emphasize promising findings without adequately acknowledging the many remaining challenges [19].

Embryonic and other types of stromal cells have tumorigenic potential and have been proposed as a source of common origin for cancer [20]. Embryonic stem cells form teratomas when injected into mice, and murine neural stem cells can transform into malignant gliomas with minimal genetic changes [21]. Furthermore, rapidly dividing cells in culture can acquire mutations that may predispose the cells to malignant transformation. This case and others in which tumors have developed in the context of stem-cell tourism [22,23] (a trend in which patients travel for the purpose of obtaining therapy) illustrate an extremely serious complication of introducing proliferating stem cells into patients. Investigators have attempted to reduce the risk of stem-cell–related tumors in clinical trials by means of the measured administration of pluripotent stem cells or by differentiating stem cells in vitro into postmitotic phenotypes before administration [24,25].

Although there may be some concern about mesenchymal stem/stromal cells (MSCs) tumorigenicity—mainly in the breast cancer field—the in vivo evidence collected so far remains inconclusive [26]. In a recent clinical study, autologous MSCs from cancer patients were locally administered at the site of a

malignant primary bone tumor resection, and no increase in the cancer local recurrence risk was shown after an average follow-up of 15 years [27]. We performed an autologous bone marrow–derived MSC transplantation in a 42-year-old man with a broncho-pleural fistula after right extrapleural pneumonectomy for malignant mesothelioma [18]. The 2-year follow up by whole-body computed tomography scan, positron emission tomography, and flexible bronchoscopy did not show any recurrence or neoplastic findings neither within the bronchial stump—where the MSCs were injected—nor outside the chest. From the cell manufacturing standpoint, the production process and quality assessment were designed to preserve the safety of the final cell product and included an in-depth cell growth evaluation, a short (one-passage) culture time, and a complete karyotype assessment before product release. Although we fully agree on the need for further experimental and clinical protocols on MSC therapy for airway restoration in oncologic patients, we believe that—in case of bronchogenic carcinoma—the only clear contraindication to MSC local injection remains local residual tumor [28].

5.10 Significance and innovation

The main function of stem/progenitor cells for the airway epithelium is epithelial homeostasis and the repair of defects in the airway wall . Stem/progenitor cells can be used to repair defects in the airway wall, resulting from tumors, trauma, tissue reactions following long-time intubations, or diseases that are associated with epithelial damage. Reconstruction of tracheobronchial defects requires in the first place the availability of airway epithelial cells and the presence of fibroblasts or fibroblast-derived substances. The fact that fibroblasts have positive effects on airway epithelial cell growth emphasizes the fact that the airway is not a simple structure and that epithelial-mesenchymal interactions are important [28]. The crucial innovation of our model is the synergistic approach by AMSC bronchoscopic transplantation and intra venous injection of GCSF, allowing a potential tissue repair by a double pathway (local and systemic), each one proven to be effective for wound healing, although never used together before and in particular for airway tissue defects restoration.

5.11 References

1. de la Portilla F, Alba F, García-Olmo D, Herrerías JM, González FX, Galindo A Expanded allogeneic adipose-derived stem cells (eASCs) for the treatment of complex perianal fistula in Crohn's disease: results from a multicenter phase I/IIa clinical trial *Int J Colorectal Dis.* 2013 Mar;28(3):313-23. doi: 10.1007/s00384-012-1581-9
2. Di Nicola M, Carlo-Stella C, Magni M et al (2002) Human bone marrow stromal cells suppress T-lymphocyte proliferation induced by cellular or nonspecific mitogenic stimuli. *Blood* 99:3838–3843
3. Doorn J, Moll G, Le Blanc K et al (2012) Therapeutic applications of mesenchymal stromal cells: paracrine effects and potential improvements. *Tissue Eng Part B Rev* 18:101–115
4. Krampera M (2011) Mesenchymal stromal cell ‘licensing’: a multistep process. *Leukemia* 25:1408–1414
5. Le Blanc K, Tammik C, Rosendahl K et al (2003) HLA expression and immunologic properties of differentiated and undifferentiated mesenchymal stem cells. *Exp Hematol* 31:890–896
6. Mitchell JB, McIntosh K, Zvonic S et al (2006) Immunophenotype of human adipose-derived cells: temporal changes in stromal-associated and stem cell-associated markers. *Stem Cells* 24:376–385
7. Gonzalez-Rey E, Anderson P, González MA et al (2009) Human adult stem cells derived from adipose tissue protect against experimental colitis and sepsis. *Gut* 58:929–939
8. González MA, Gonzalez-Rey E, Rico L et al (2009) Adipose derived mesenchymal stem cells alleviate experimental colitis by inhibiting inflammatory and autoimmune responses. *Gastroenterology* 136:978–989
9. Garcia-Olmo D, Garcia-Arranz M, Garcia LG et al (2003) Autologous stem cell transplantation for treatment of rectovaginal fistula in perianal Crohn's disease: a new cell-based therapy. *Int J Colorectal Dis* 18:451–454
10. Garcia-Olmo D, Garcia-Arranz M, Herreros D et al (2005) A phase I clinical trial of the treatment of Crohn's fistula by adipose mesenchymal stem cell transplantation. *Dis Colon Rectum* 48:1416–1423

11. Garcia-Olmo D, Herreros D, Pascual I et al (2009) Expanded adipose-derived stem cells for the treatment of complex perianal fistula: a phase II clinical trial. *Dis Colon Rectum* 52:79–86
12. Ciccocioppo R, Bernardo ME, Sgarella A et al (2011) Autologous bone marrow-derived mesenchymal stromal cells in the treatment of fistulising Crohn's disease. *Gut* 60:788–798
13. Haas R, Murea S (1995) The role of granulocyte colony-stimulating factor in mobilization and transplantation of peripheral blood progenitor and stem cells. *Cytokines Mol Ther* 1:249–270
14. Baldo MP, Davel APC, Damas-Souza DM, Nicoletti-Carvalho JE, Bordin S, Carvalho HF, Rodrigues SL, Rossoni LV, Mill JG (2011) The antiapoptotic effect of granulocyte colony-stimulating factor reduces infarct size and prevents heart failure development in rats. *Cell Physiol Biochem* 28:33–40
15. Cho S-W, Lim JE, Chu HS, Hyun H-J, Choi CY, Hwang K-C, Yoo KJ, Kim D-I, Kim B-S (2006) Enhancement of in vivo endothelialization of tissue-engineered vascular grafts by granulocyte colony-stimulating factor. *J Biomed Mater Res A* 76:252–263
16. Liongue C, Wright C, Russell AP, Ward AC (2009) Granulocyte colony-stimulating factor receptor: stimulating granulopoiesis and much more. *Int J Biochem Cell Biol* 41:2372–2375
17. Petrella F, Toffalorio F, Brizzola S, De Pas TM, Rizzo S, Barberis M, Pelicci P, Spaggiari L, Acocella F Stem cell transplantation effectively occludes broncho-pleural fistula in an animal model *Ann Thorac Surg.* 2014 Feb;97(2):480-3.
18. Petrella F, Spaggiari L, Acocella F, Barberis M, Bellomi M, Brizzola S, Donghi S, Giardina G, Giordano R, Guarize J, Lazzari L, Montemurro T, Pastano R, Rizzo S, Toffalorio F, Tosoni A, Zanotti M Airway fistula closure after stem-cell infusion *N Engl J Med.* 2015 Jan 1;372(1):96-7.
19. Taylor-Weiner H, Graff Zivin J Medicine's Wild West--Unlicensed Stem-Cell Clinics in the United States *N Engl J Med.* 2015 Sep 10;373(11):985-7
20. Berkowitz AL, Miller MB, Mir SA, Cagney D, Chavakula V, Guleria I, Aizer A, Ligon KL, Chi JH Glioproliferative Lesion of the Spinal Cord as a Complication of "Stem-Cell Tourism" *N Engl J Med.* 2016 Jun 22

21. Bachoo RM, Maher EA, Ligon KL, et al. Epidermal growth factor receptor and Ink4a/Arf: convergent mechanisms governing terminal differentiation and transformation along the neural stem cell to astrocyte axis. *Cancer Cell* 2002; 1: 269-77
22. Thirabanasak D, Tantiwongse K, Thorner PS. Angiomyeloproliferative lesions following autologous stem cell therapy. *J Am Soc Nephrol* 2010; 21: 1218-22.
23. Amariglio N, Hirshberg A, Scheithauer BW, et al. Donorderived brain tumor following neural stem cell transplantation in an ataxia telangiectasia patient. *PLoS Med* 2009; 6(2): e1000029.
24. Mazzini L, Gelati M, Profico DC, et al. Human neural stem cell transplantation in ALS: initial results from a phase I trial. *J Transl Med* 2015; 13: 17.
25. Fox IJ, Daley GQ, Goldman SA, et al. Use of differentiated pluripotent stem cells as replacement therapy for treating disease. *Science* 2014; 345(6199): 127391.
26. Mazzini L, Gelati M, Profico DC, et al. Human neural stem cell transplantation in ALS: initial results from a phase I trial. *J Transl Med* 2015; 13: 17.
27. Fox IJ, Daley GQ, Goldman SA, et al. Use of differentiated pluripotent stem cells as replacement therapy for treating disease. *Science* 2014; 345(6199): 127391.
28. Petrella F, Rizzo S, Borri A, Casiraghi M, Spaggiari L. Current perspectives in mesenchymal stromal cell therapies for airway tissue defects. *Stem Cells Int* 2015;2015:746392.

5.12 Figure Legend

Figure 1: centrifugated abdominal lipoaspirate (2500 rotations x 2 minutes)

Figure 1: centrifugated abdominal lipoaspirate (2500 rotations x 2 minutes)

